Can nano-particles of Ice and Dust affect the Charge-Exchange X-ray emission?

V. Kharchenko

Harvard-Smithsonian CfA & *University of Connecticut*

1. Nano-particles in Astrophysical Environments
2. Interaction between nano-particles and astrophysical plasmas
3. Nucleation of nano-scale dust, ice, and haze particles around ion seeds. Size distribution of nano-particles
4. Charge exchange, scattering, and fluorescence phenomena for nano-scale objects
5. Multi-channel collisions between ions and nano-particles and charge-exchange. Fragmentation of nano-particles
6. Theory and experiments on charge-exchange processes in collisions between highly charged ions and nano-particles

Submicron Particles in Astrophysical Environments

<u>Nano-particles</u>: Interstellar dust, Cometary ice and dust, Noctilucent clouds, Exoplanetary dust and haze, aerosols etc.

Circumstellar Dust in Accretion Disks

Example: Accretion disk of the red dwarf AU Mic .
Webb observations. Very strong stellar wind.

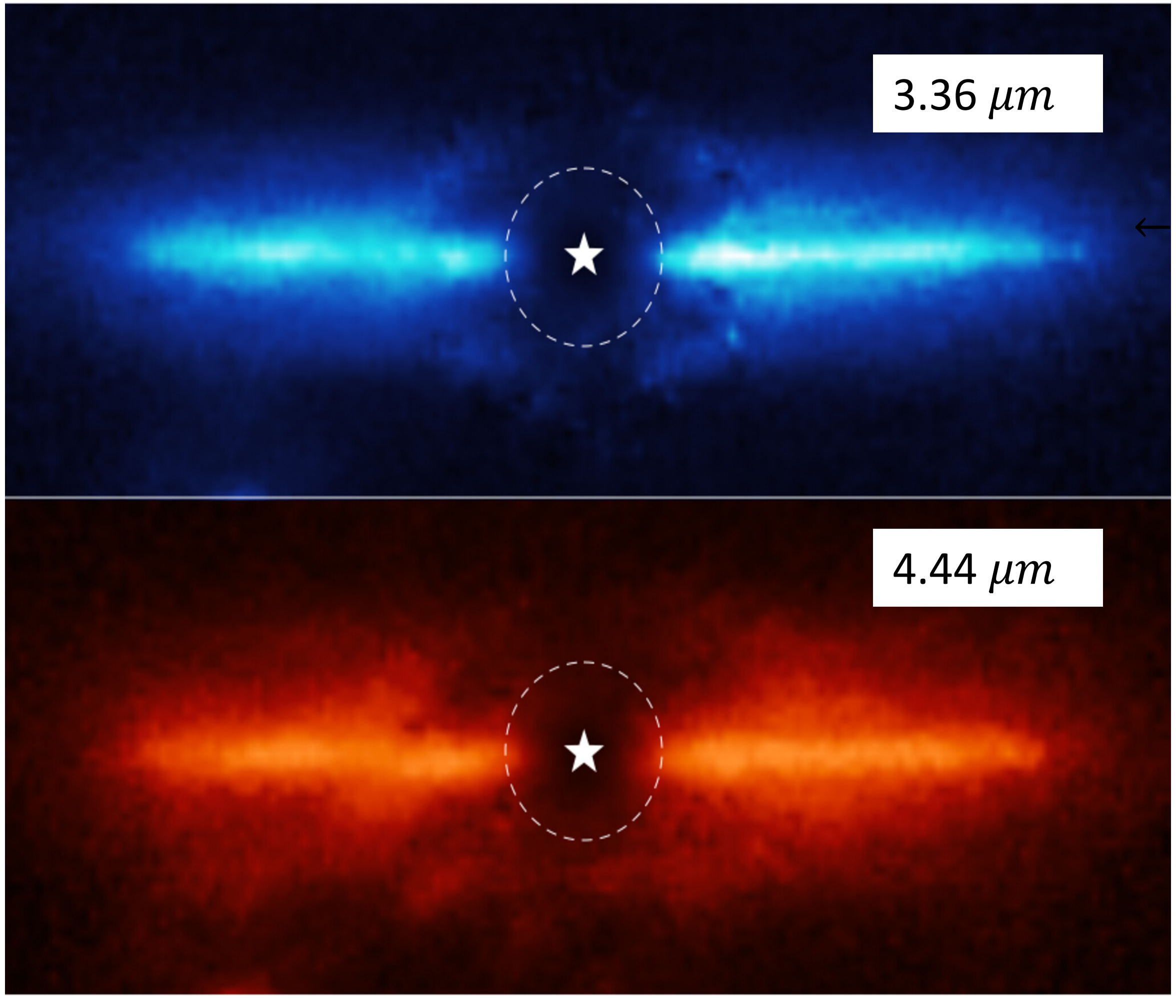

Zodiacal Dust

Scattering and fluorescence of the Solar Radiation.
CX, Neutral Wind, and X-rays: Kharchenko and Lewkow (2012, Springer}

Cometary Dust and Ice Particles, Exoplanetary Atmospheric Haze, Aerosols, and High Altitude Clouds

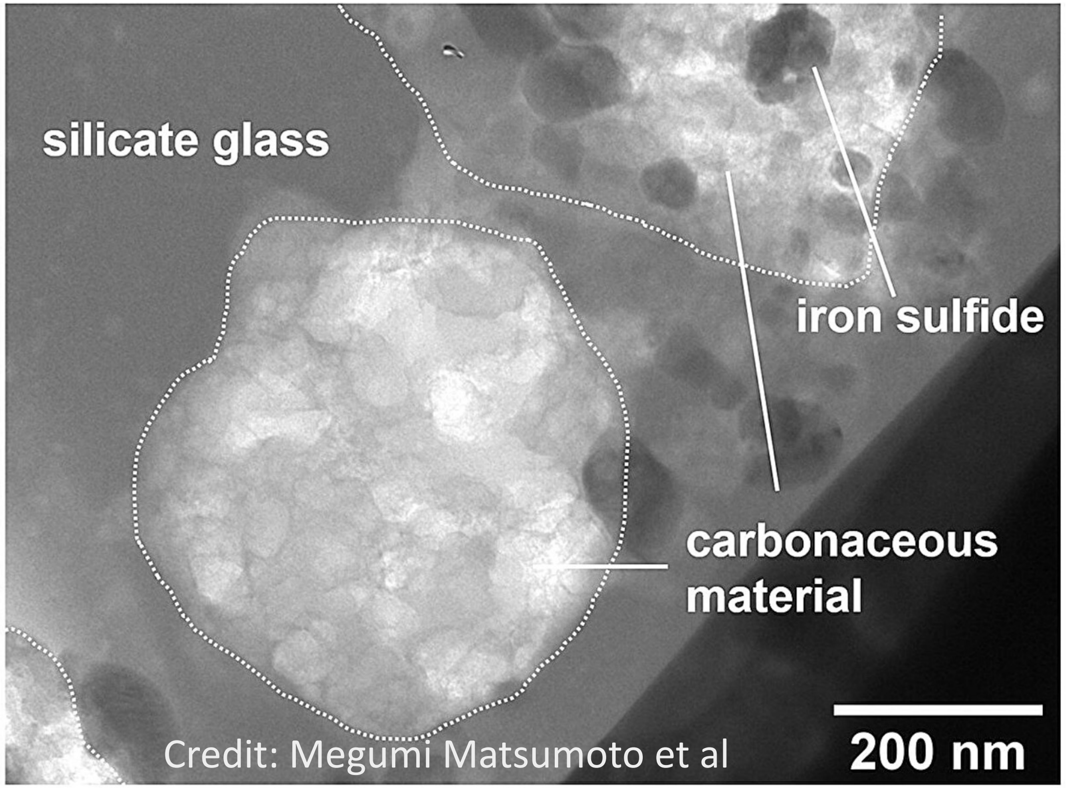

Cometary Dust

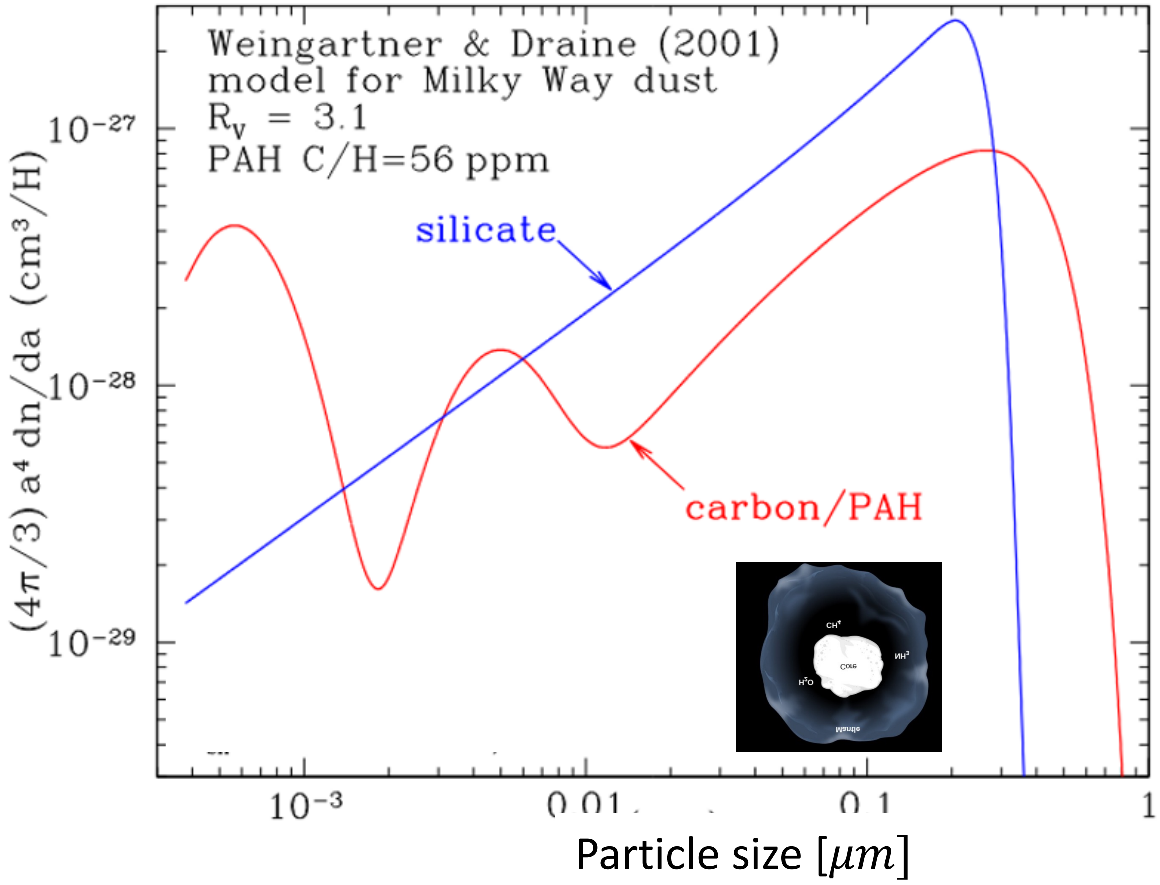

Interstellar Dust

Charge Transfer Collisions between Nanoparticles and Ions : Hybrid Model

(This equation is valid for the single electron capture in quasi-elastic collisions between ion and nanoparticle)

$$\sigma_{CX}(a, E, I_p) = \frac{\pi}{2}\left[a + (1 + 2\sqrt{q})\frac{e^2}{I_p} + \left(\frac{\hbar^2}{2m_e I_p}\right)^{\frac{1}{2}}\left(\ln\left(\sqrt{\frac{E_0}{E}}\right) + A_q\right)\right]^2,$$

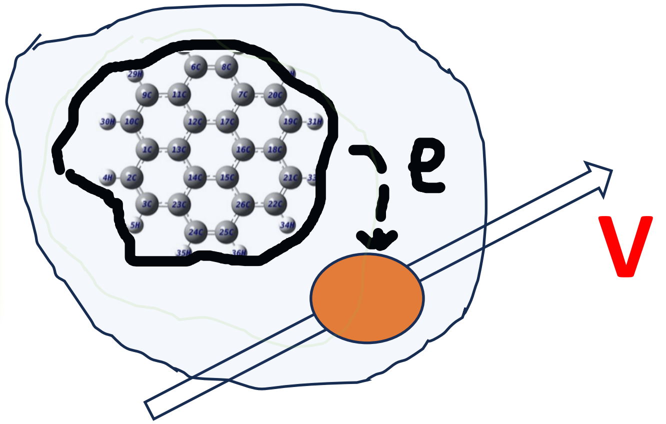

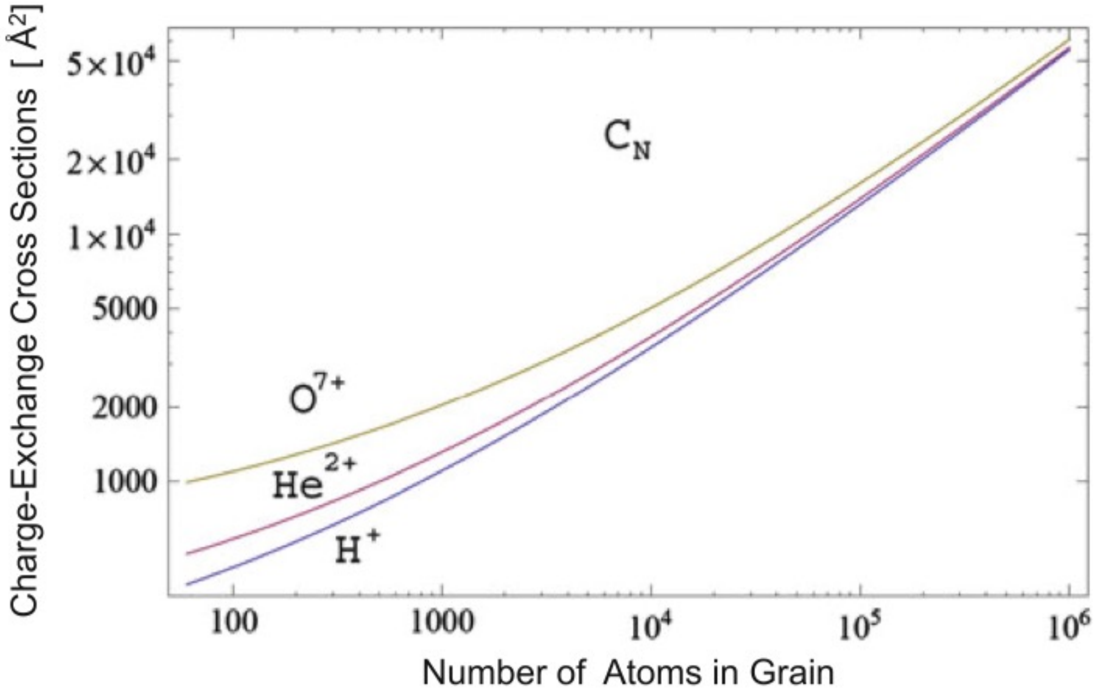

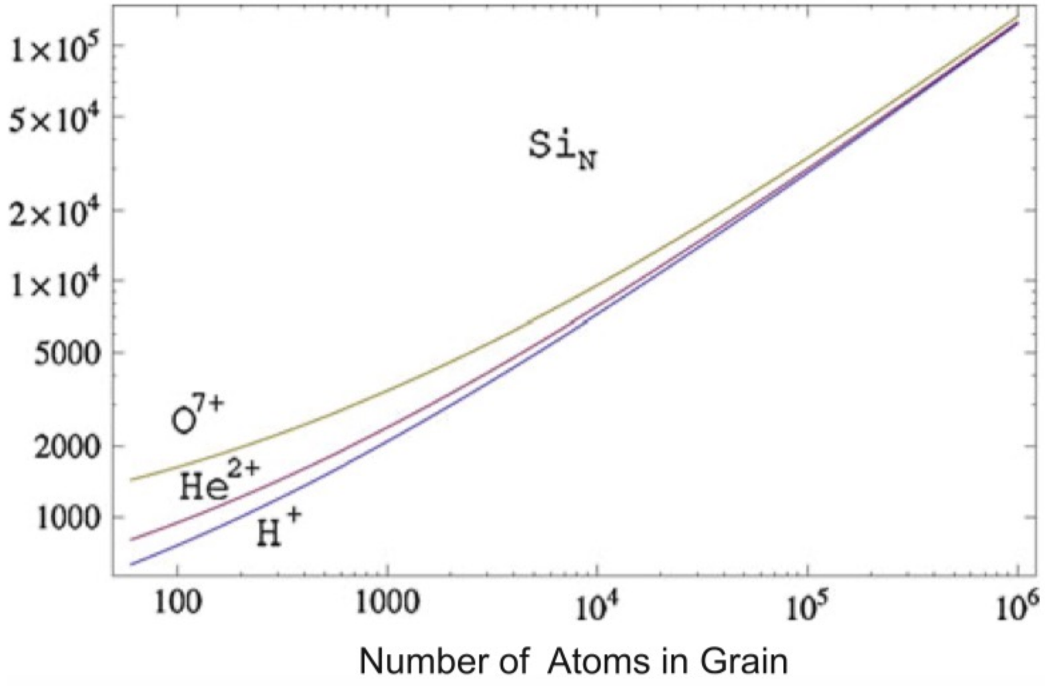

Contribution of Zodiacal Dust into the local X-ray background

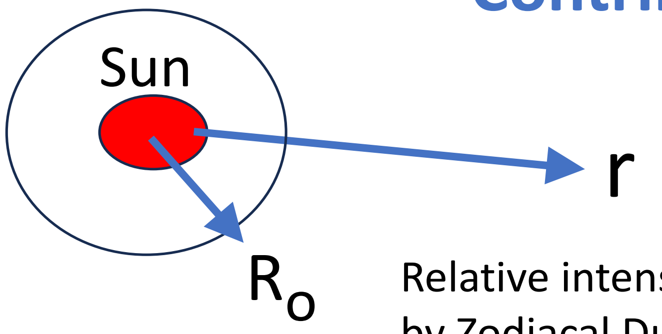

Relative intensity of X-rays I_Z/I_0 induced by Zodiacal Dust for photons with different energies:

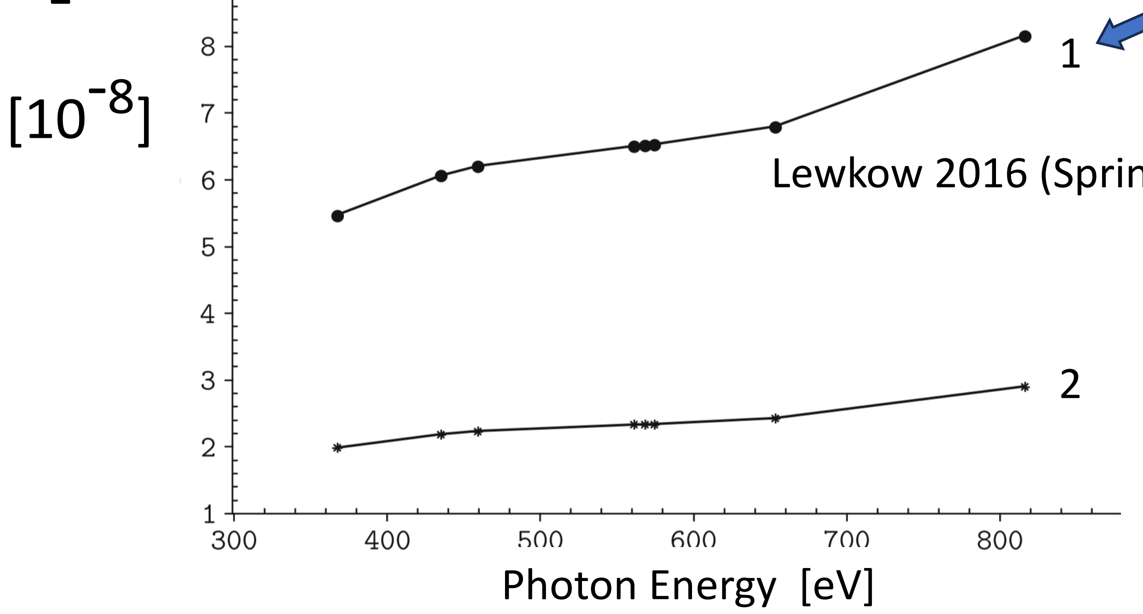

The estimated value of the total X-ray flux from grains is smaller two orders of magnitude than the X-ray background emission. It can be seen during X-ray Solar Flares.

Size Distribution of nano-particle radius *"a"*:

(Czechowski, A. and Mann, I.: 2012)

$$\frac{\partial n(r,a)}{\partial a} \simeq 2.5 n_{\mathrm{d}}(R_0)\, \frac{a_{\min}^{3.5}}{a^{3.5}} \left(\frac{R_0}{r}\right)^2$$

where

Ro=1AU; $n_d(R_0)=1.5 * 10^{-10}$ cm-3 ,

and $I_0(\hbar\omega)$ is the photon flux at Ro

Nano-size dust particles can be trapped in the region ~ (0.1 - 0.2) Ro and CX collisions between ions SW and nano particles may create neutral SW wind of H and He +:

$$\Gamma(\mathrm{He}^+) = < n_{\mathrm{d}}(r,a)\sigma_{\mathrm{CX}}^{\mathrm{He}^+}(a) >_{r,a} = 1.7 \times 10^{-21} \mathrm{cm}^{-1}$$

In situ satellite observations: $4.6 * 10^{-21}$ cm^{-1} (Collier et al. 2003).

Cometary X-rays above 1Kev: Possible Contribution of the Dust/ Gas Scattering

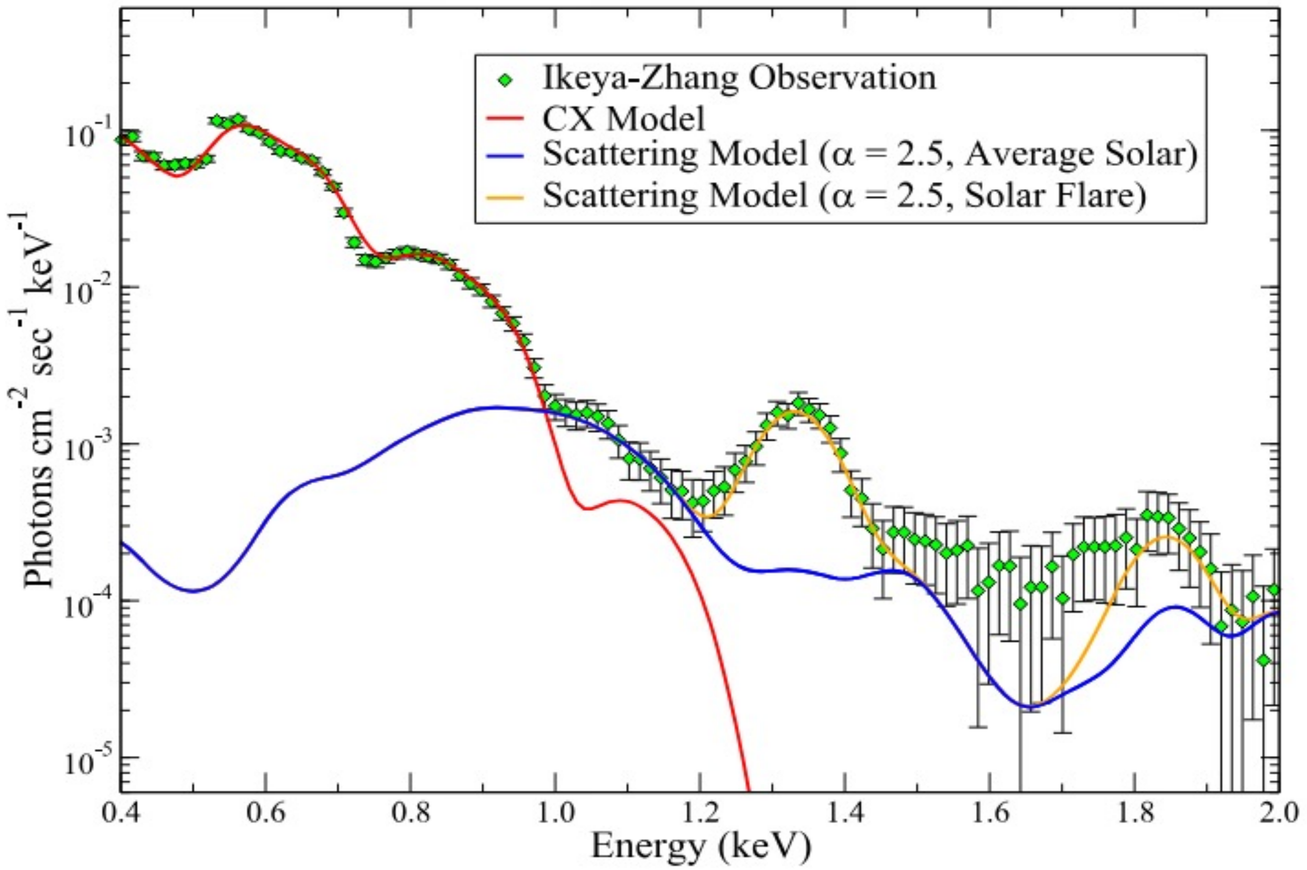

Figure 1. Comparison of the modeled spectral intensity contributions from CX and dust/ice particle scattering to the *Chandra* observation of Comet Ikeya–Zhang. The modeled scattering emission includes dust contribution from all grain radii. The scattering model is calculated for both the average solar and solar flare spectrum, with the solar flare spectrum producing an excellent agreement to the observation at energies greater than 1 keV.

Snios et al. ApJ (2018)

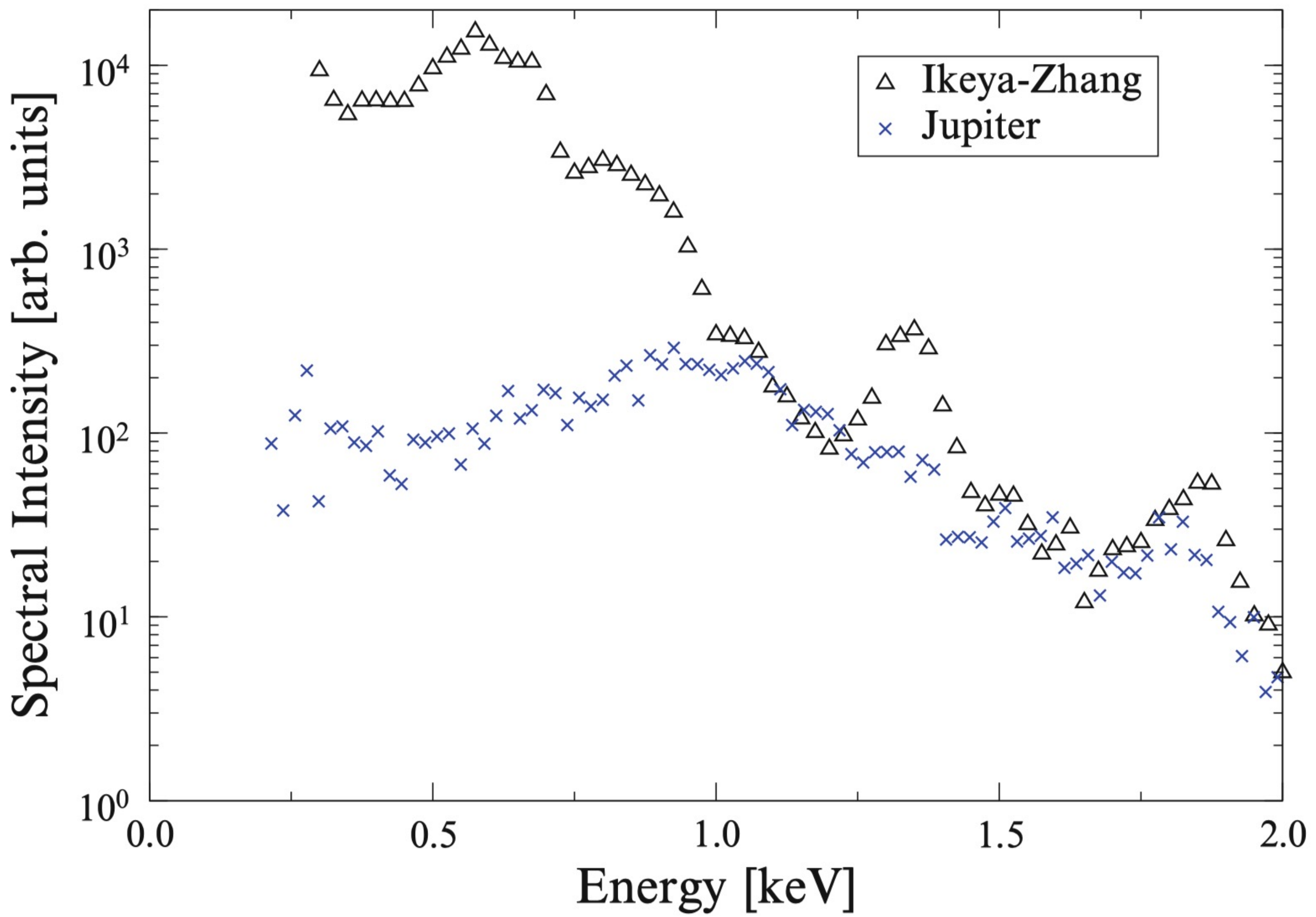

Fig. 3.11 Comparison of X-ray spectrum from comet Ikey-Zhang [10] and Jupiter [3], observed during solar X-ray flares. The data sets have been scaled to overlay together in order to better visualize the strong similarity in spectral structure between the two astronomical objects at photon energies above 1 keV

New Model for CX collisions between Ions and Nano-particles:

Charge Exchange in collisions of C_{60} fullerene with N^+ ions (Experiment and Theory)

$C_{60} + N^+ \rightarrow N + C_{60-2m} + m * C_2$

m – the number of ejected C_2 molecules

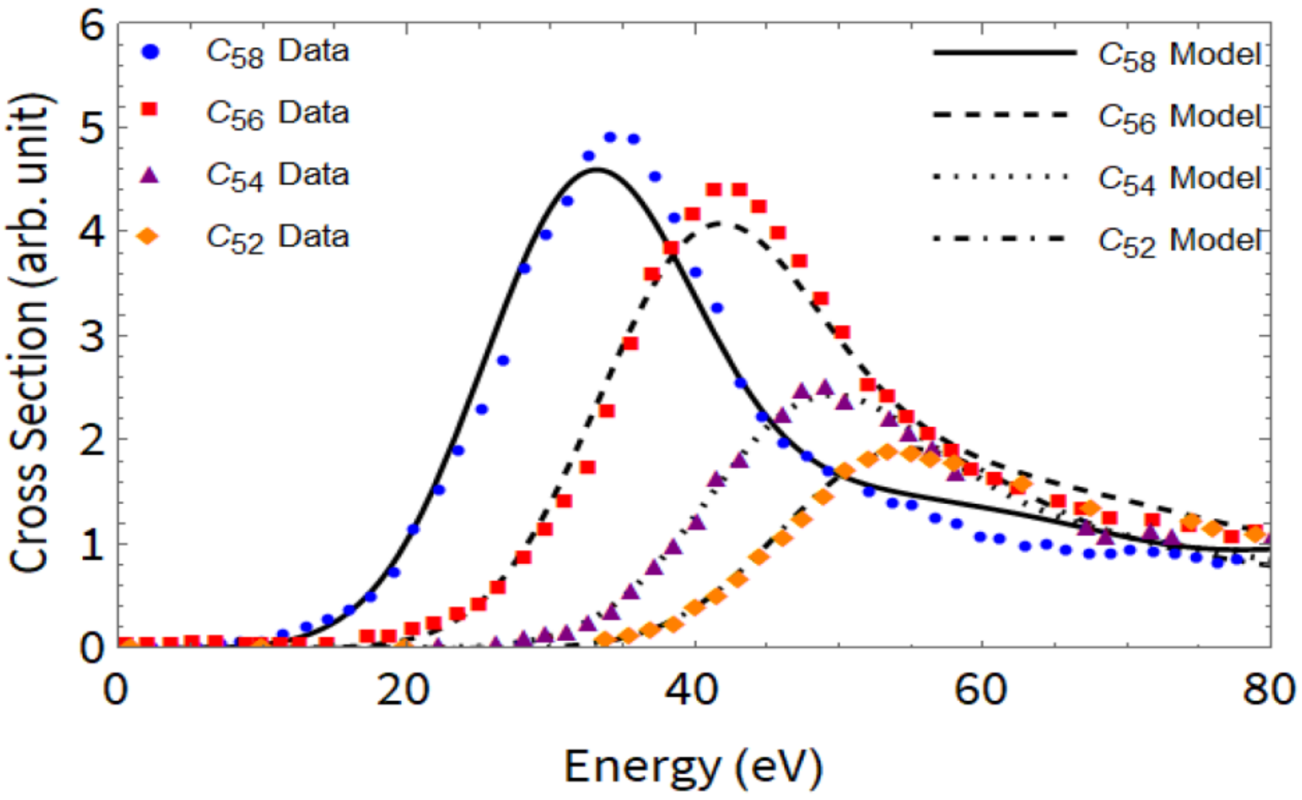

FIGURE 6.7: The experimental cross sections[3] for C_{60} colliding with N^+ (shown as the circular, square, triangular and diamond points) plotted along side our model (shown in black).

Experiment: Christian et al. , J. Phys. Chem. 96, 10597 (1992)

Theory: Smucker et. al , J. Chem. Phys.,v157, 054303 (2022)

Charge Exchange collisions between C_{60} fullerene and O^+ ion: Experiment and Theory

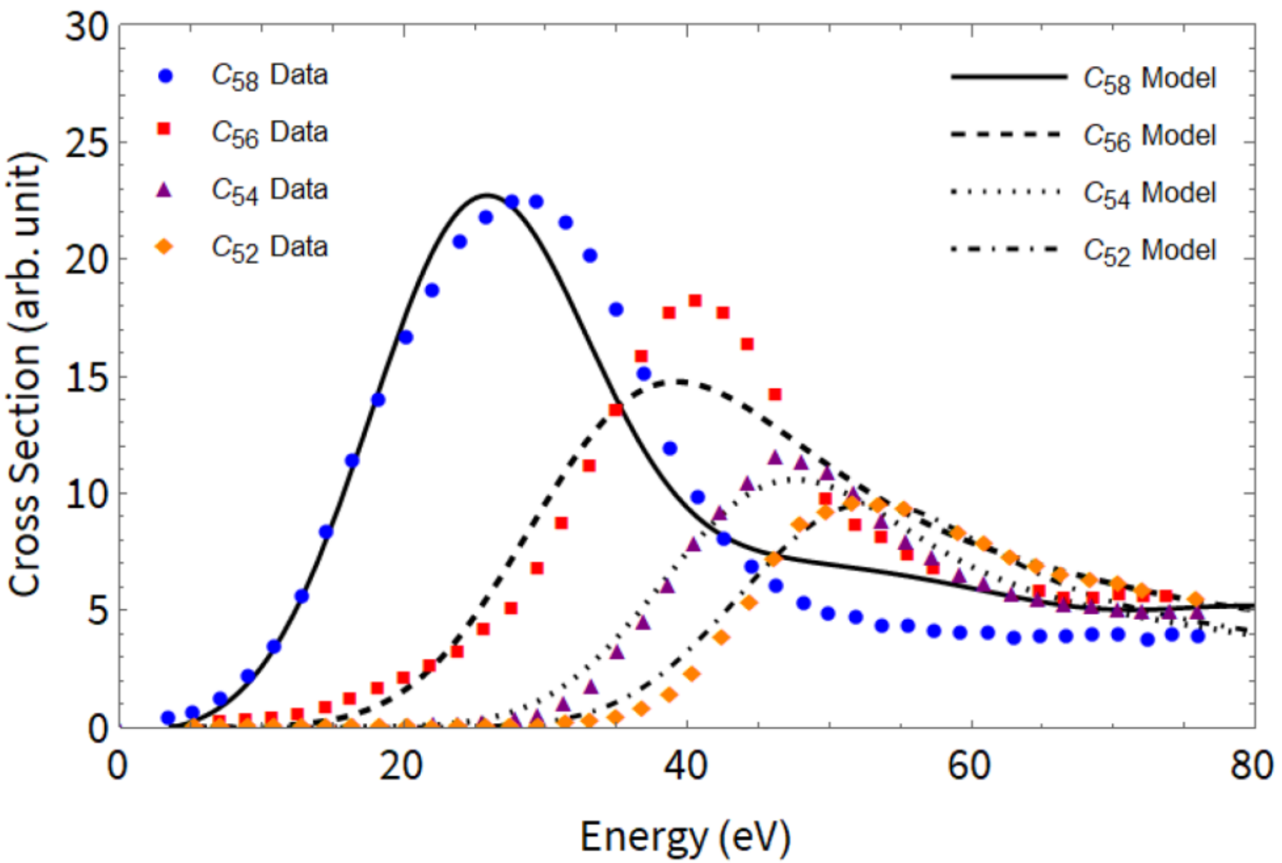

FIGURE 6.6: The experimental cross sections[4] for C_{60} colliding with O^+ (shown as the circular, square, triangular and diamond points) plotted along side our model (shown in black).

Experiment: Christian et al. , Chem. Phys. Lett. 199, 373 (1992)   Theory: Smucker et. al , J. Chem. Phys.,v157, 054303 (2022)

Multi-electron Capture in Collisions of Nano-Particles and Highly Charged Ions

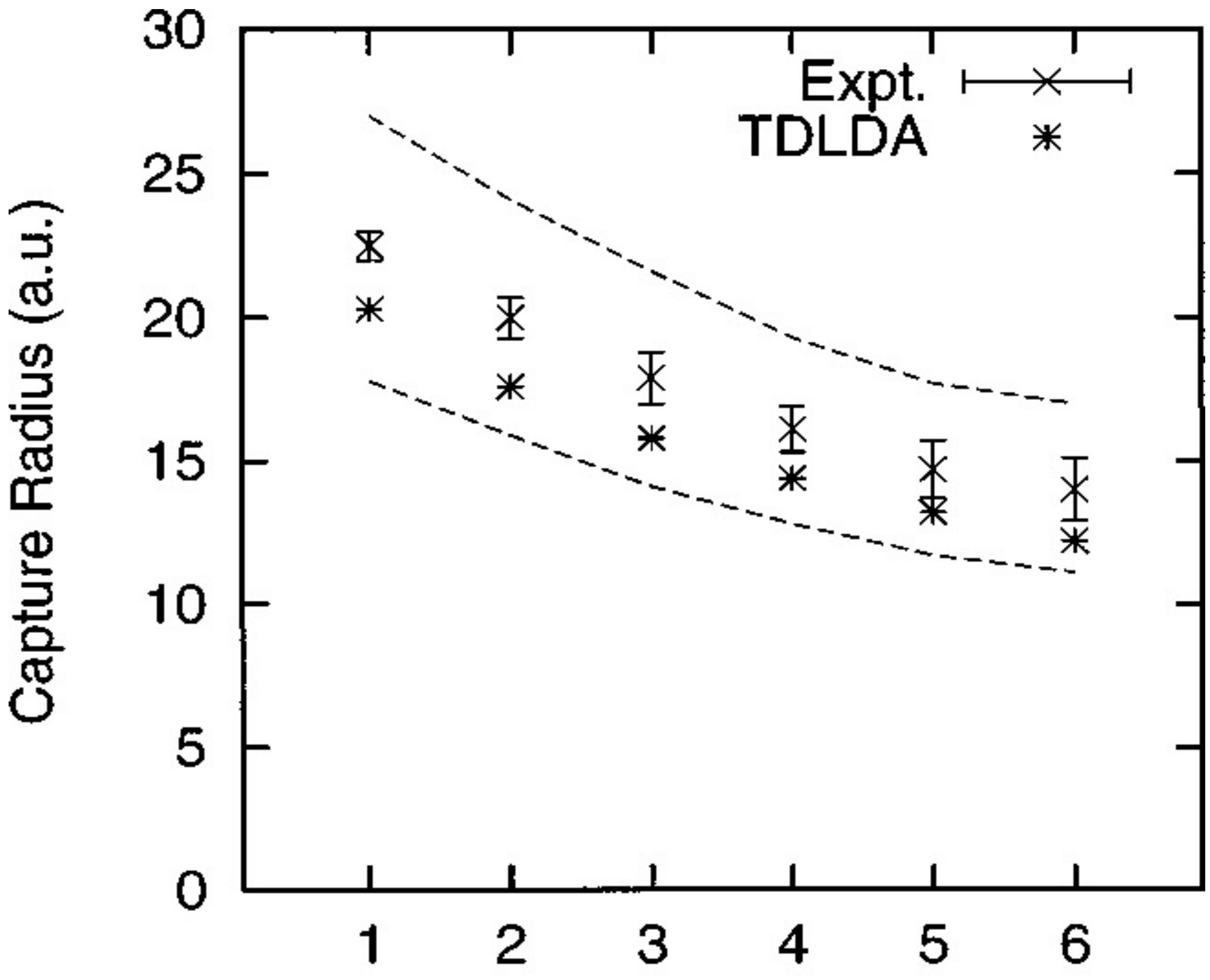

Ion charge after collision

$C_{60} + Ar^{8+} \;->\; Ar^{*(8-m)+} + \ldots$

Experimental data :
Walch et al. Phys.Rev.Lett, v72 (1994)
Theoretical results:
Yabana et al. Phys.Rev.A, v57 (1998)

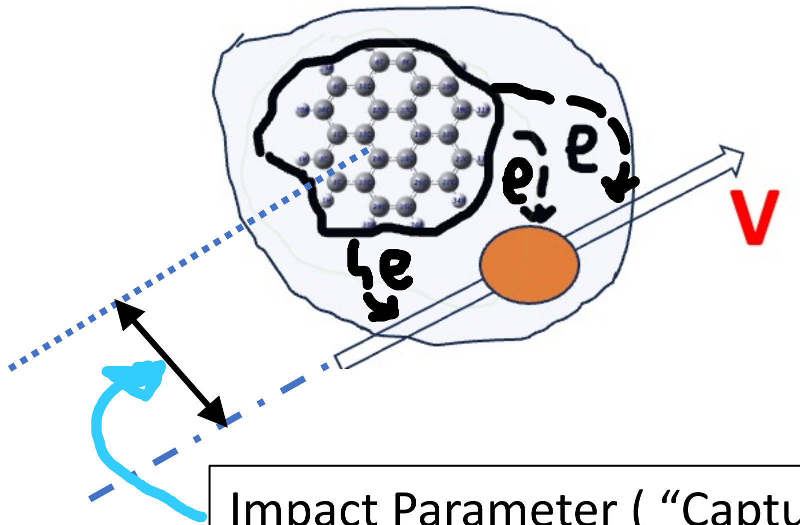

Impact Parameter ("Capture Radius")

Stripping of O and S ions in collisions with nano particles

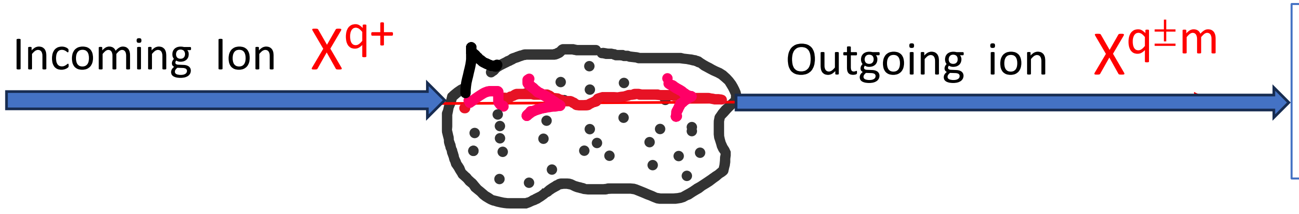

Electron capture
or
Stripping

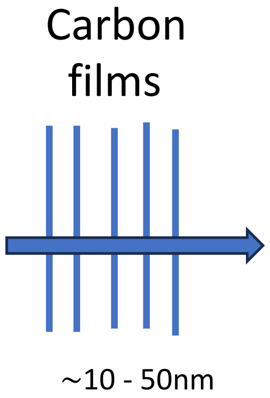

Thin films experiments

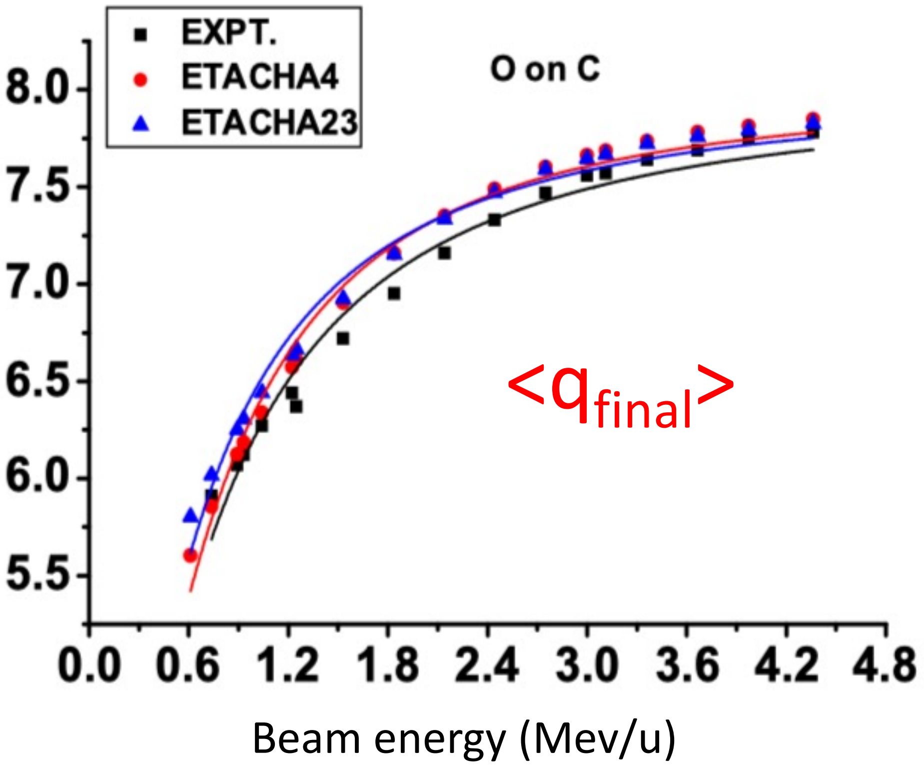

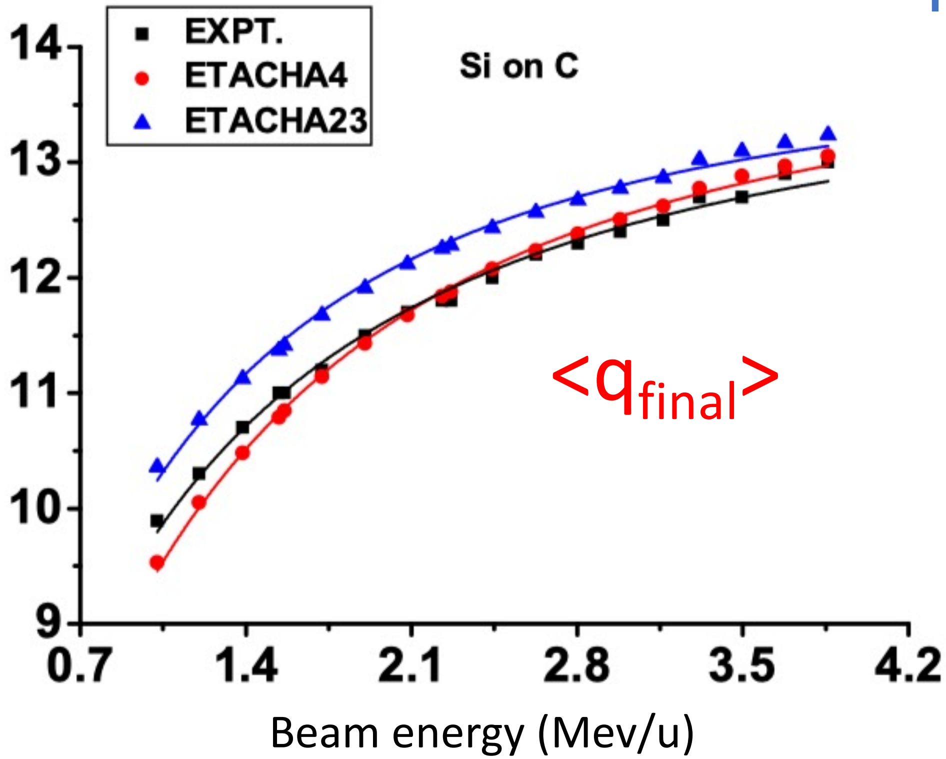

K. Shima and T. Mikumo, At. Data And Nucl. Data Tables 34, 357 (1986) ; D. Swami and T. Nandi, physics>arXiv:1709.06882 (2017)

“Highly Charged Ion – Induced Water Cluster Fragmentation “

Maisonny et al. , ICPEAC 2011, , Conference Series 388(2012)

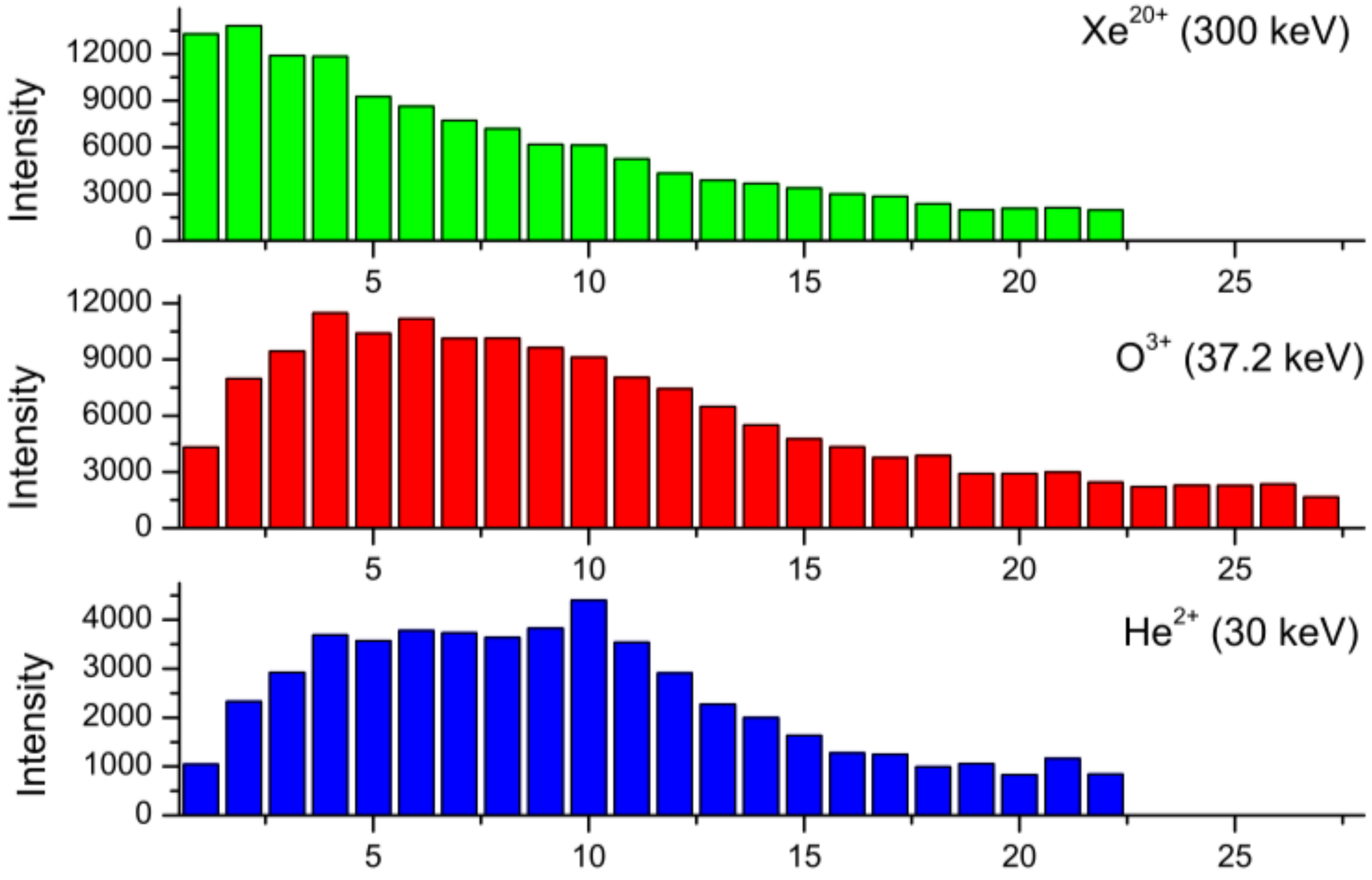

Size “n” of Water Cluster $(H_2O)_nH+$

Dynamics of nucleation and particle size distribution: Example of Ar_nH^+ nucleation

Ice Particle Nucleation and Solvation Shells

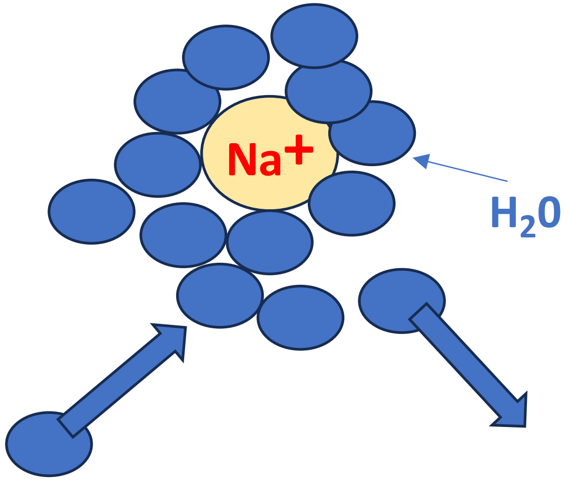

H_20

Water molecules H_20

Ion Mediated Nucleation of Ice and Haze Nano-particles

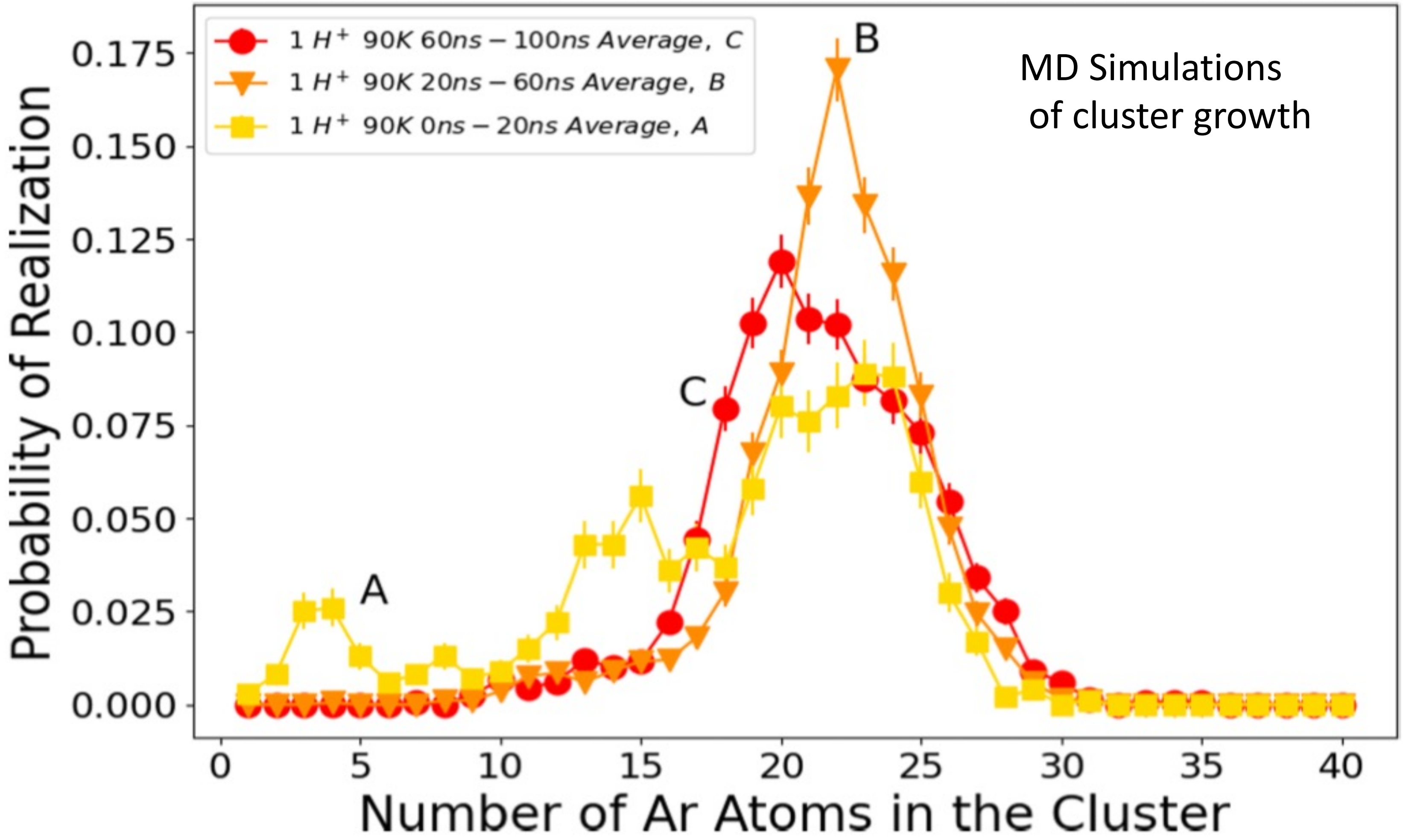

Rozman et al. Phys.Rev.A (2022)

COLLISIONAL REACTIONS: Example

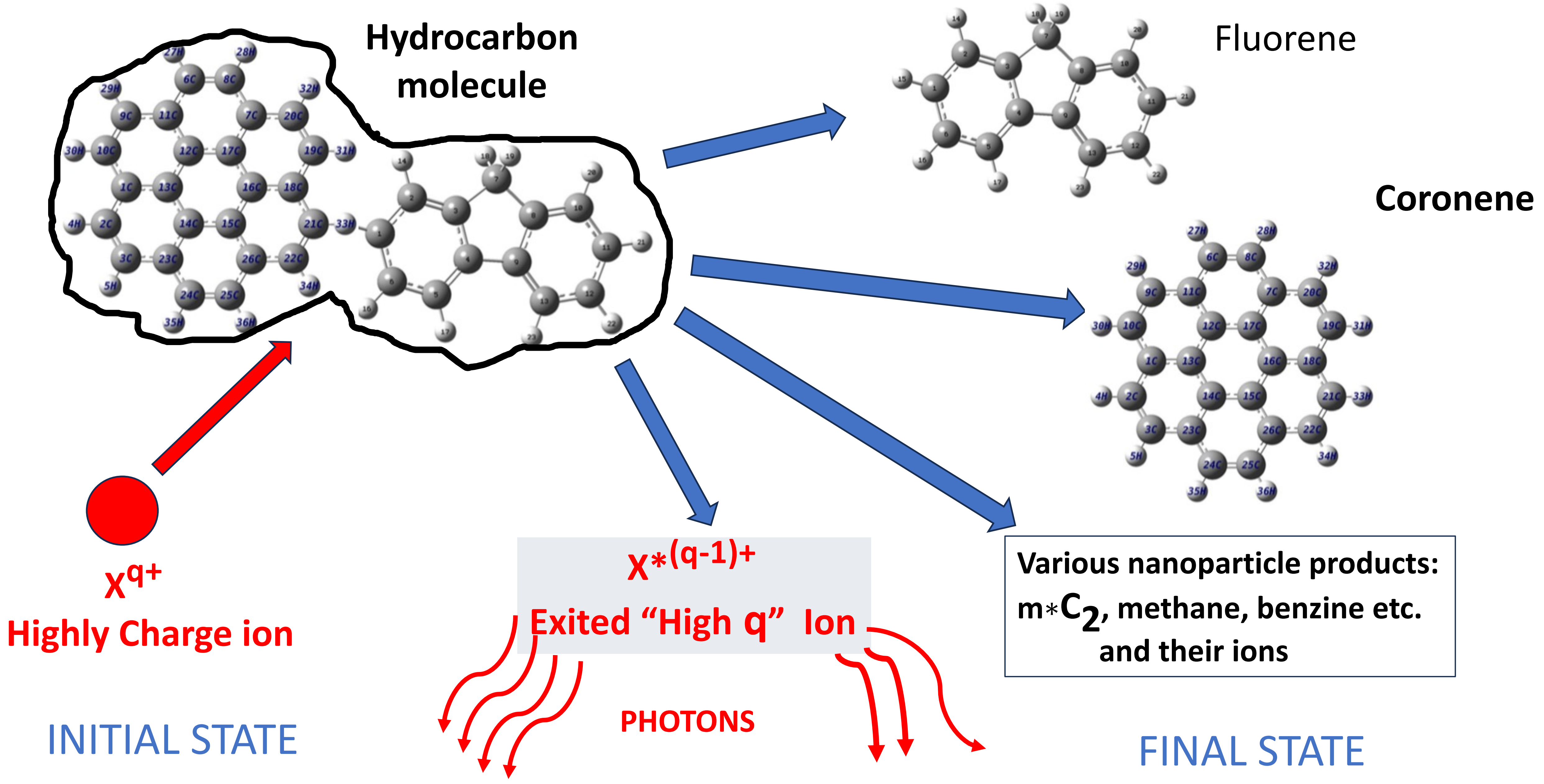

Reactive and Inelastic Collisions between Nano-Particles and Ions

<- REACTION CHANNELS ->

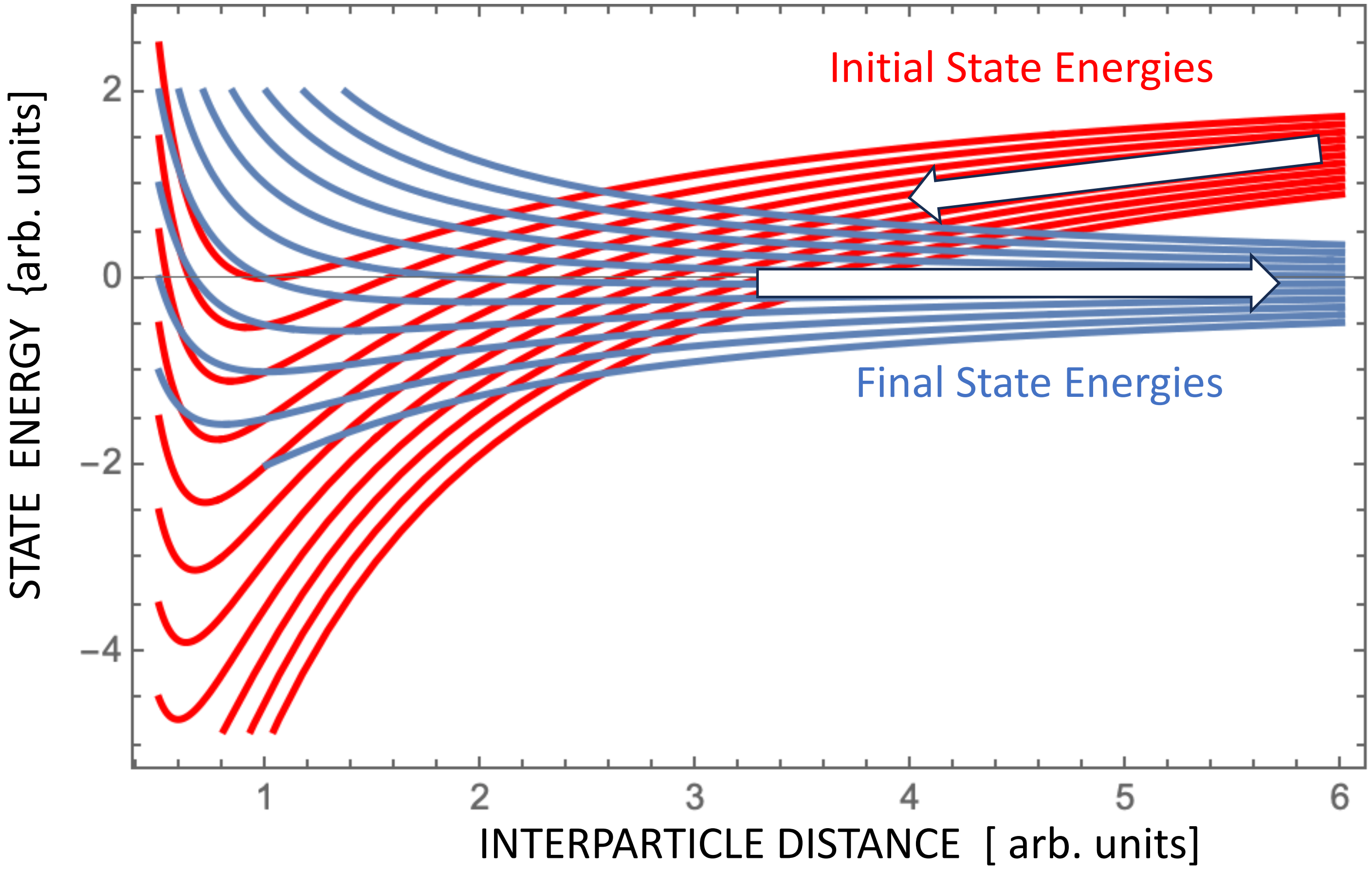

Example:

$C_{60} + X^{q+}$

$C_{60-2m} + X^{(q-1)+} + m\ {}^{*}C_2$

Initial state

Final state

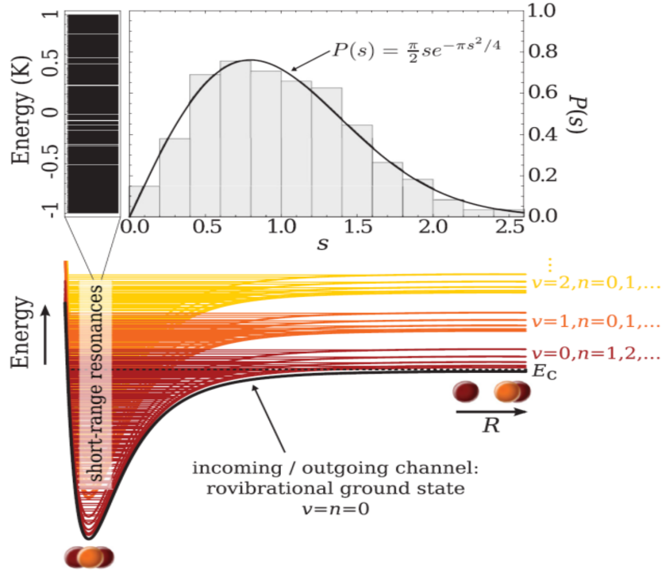

Statistical aspects of ultracold resonant scattering

Michael Mayle, Brandon P. Ruzic, and John L. Bohn

JILA, University of Colorado and National Institute of Standards and Technology, Boulder, Colorado 80309-0440, USA

State's "RANDOM WALK" during Collisions between Nano-Particles and Ions

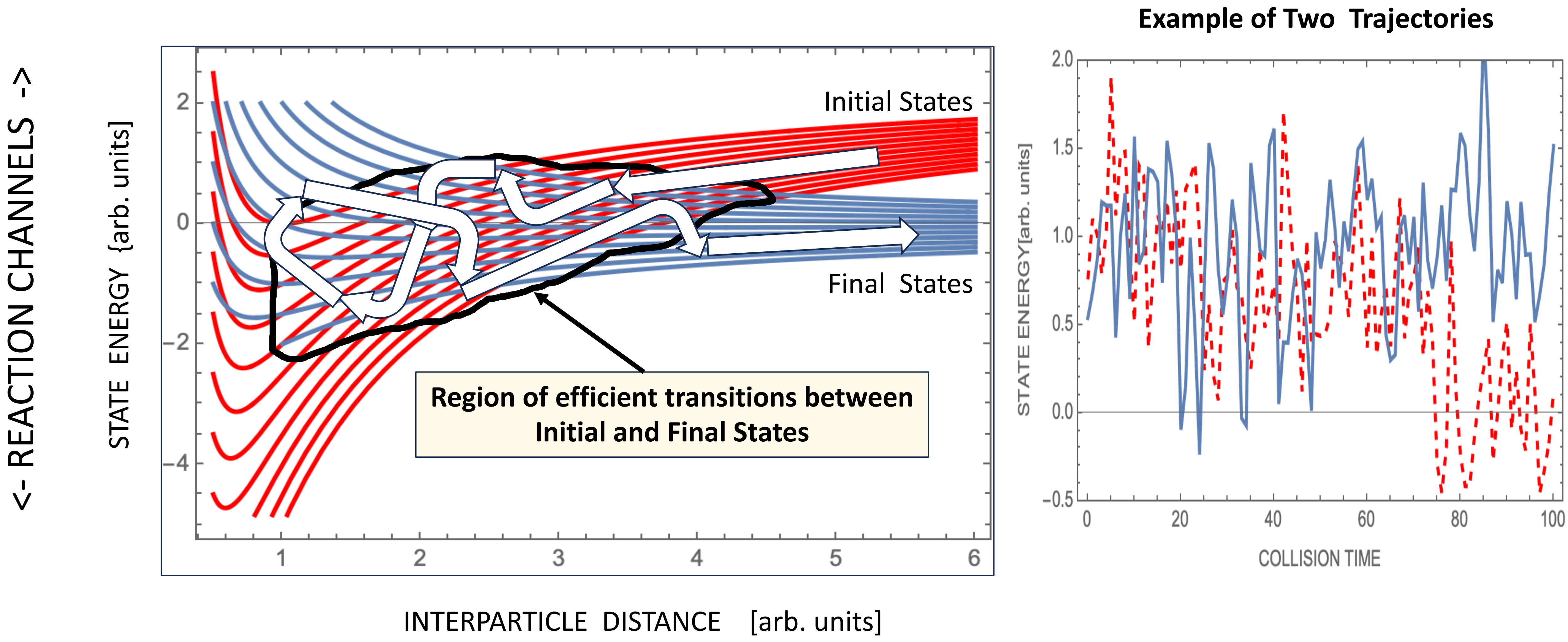

Time Evolution of State Population: From Random Walk to Diffusion in Energy Space

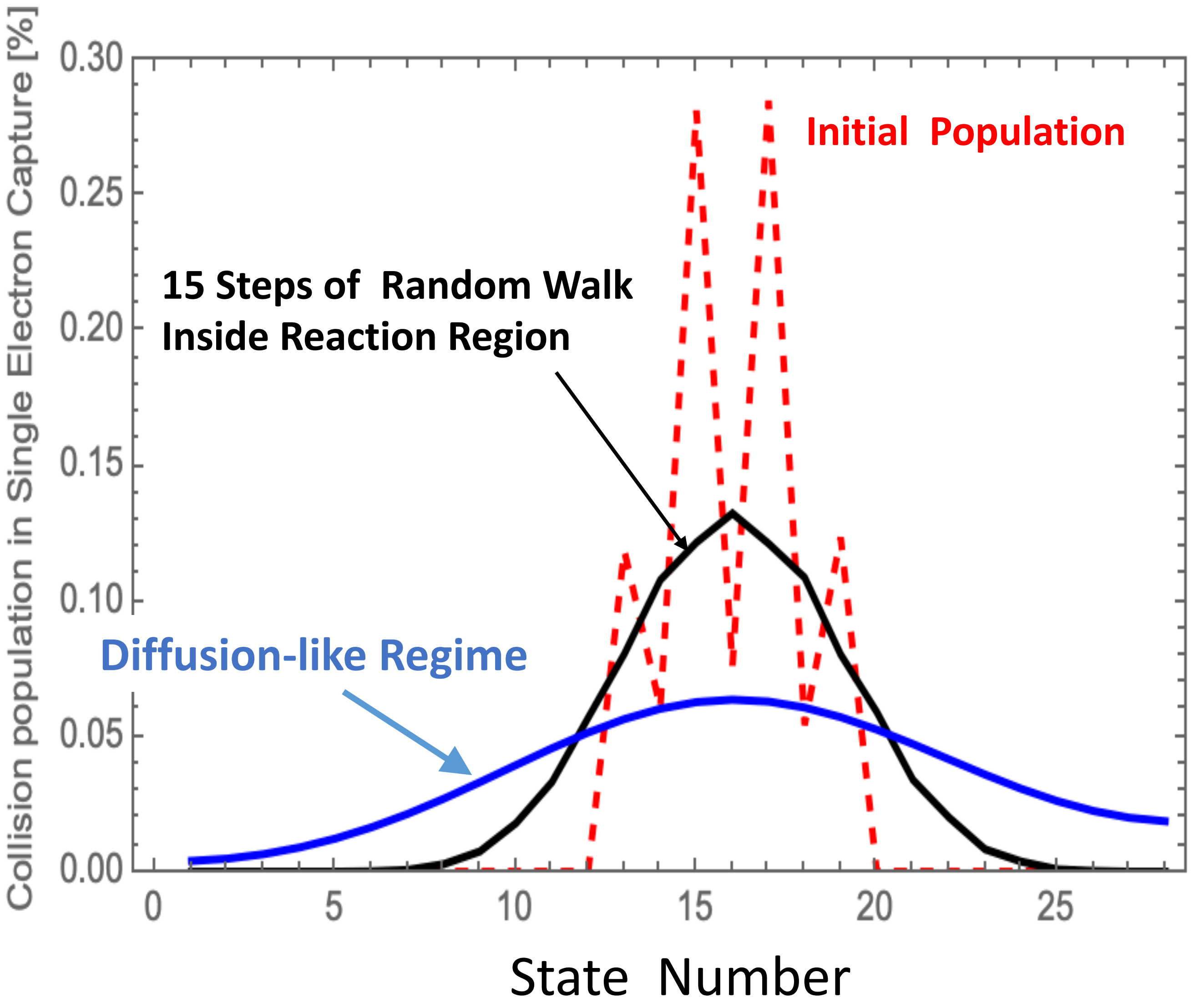

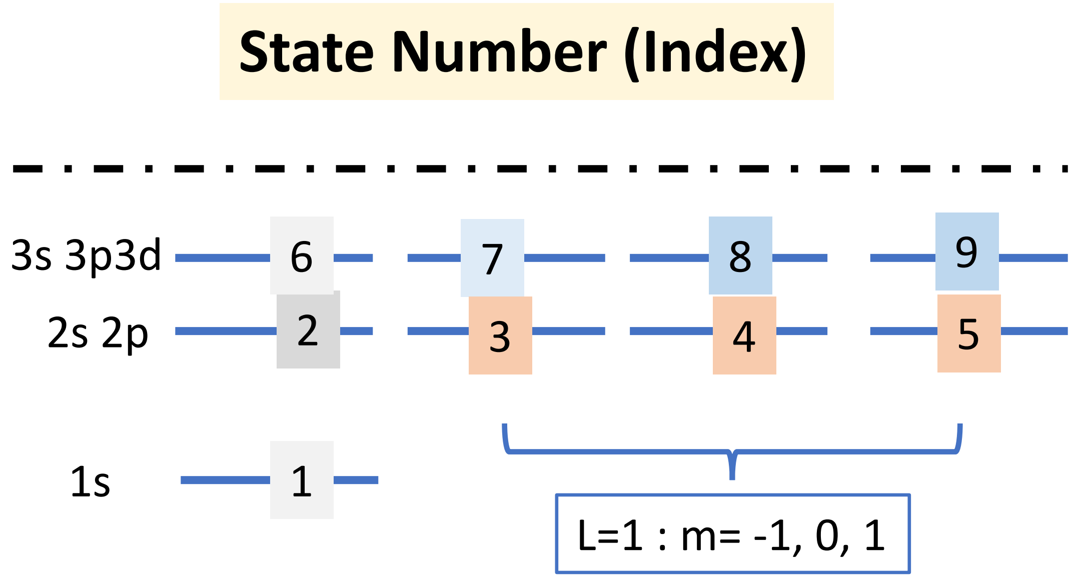

X-ray Emission Spectra Induced in the Single Electron Charge-Transfer Collisions

Simulations were performed for simplified $O^{8+} + (H_20)_n$ model

Number of molecules in the initial water cluster is n=100

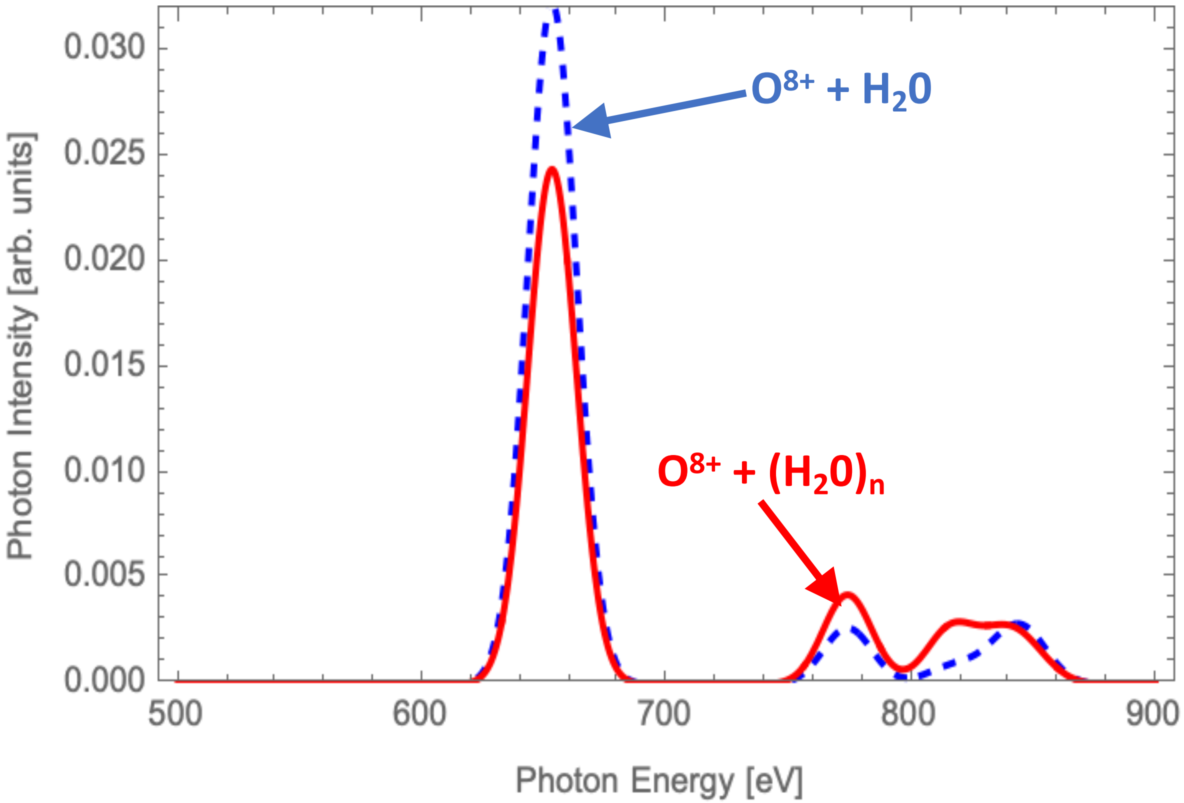

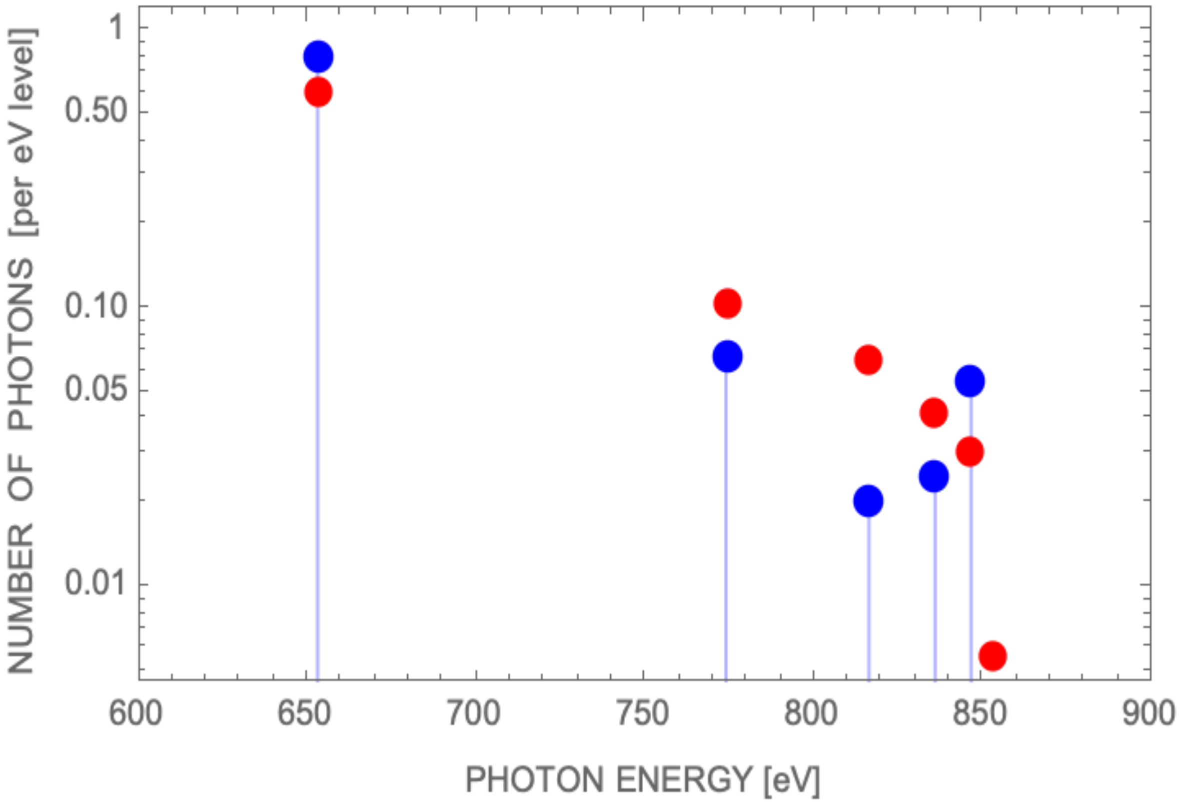

CONCLUSIONS

- Highly charged Ions can induce X-rays in collisions with dust or Ice nano-particles.
- Intensity and spectra of emitted X-rays strongly depend on collision velocity as well as on a particle size and material.
- Nano particle can be very efficient in stripping energetic ions and neutral atoms (Jupiter-like mechanism)
- Stellar or Solar Wind ions induces fragmentations of Ice/dust particles and stimulate growth of new small grains.
- Dust and Ice nano-particles can be simultaneously involved in different mechanisms of X-ray production.

Nucleation of Ar_nH^+ Nano-Clusters in Ar gas

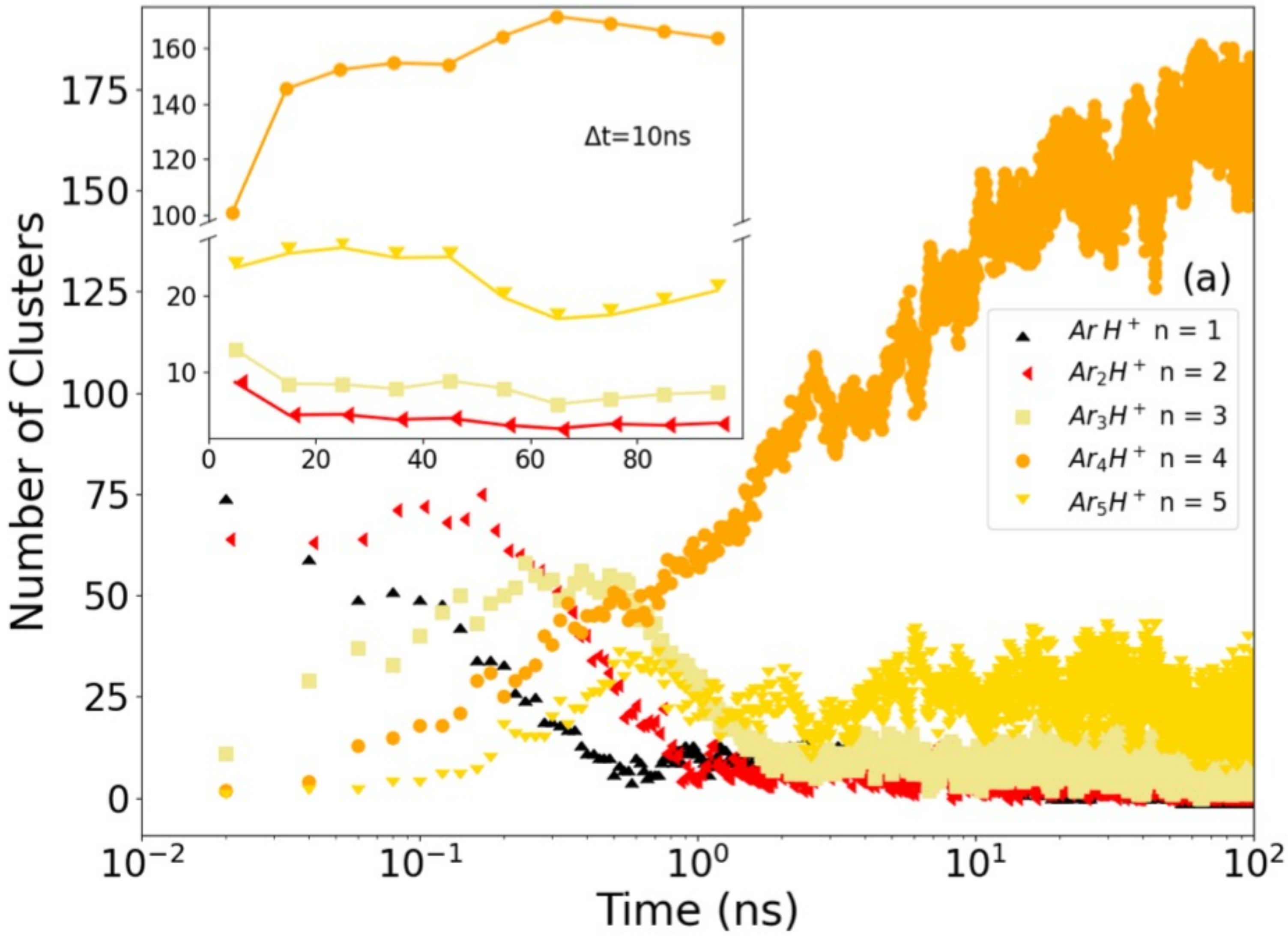

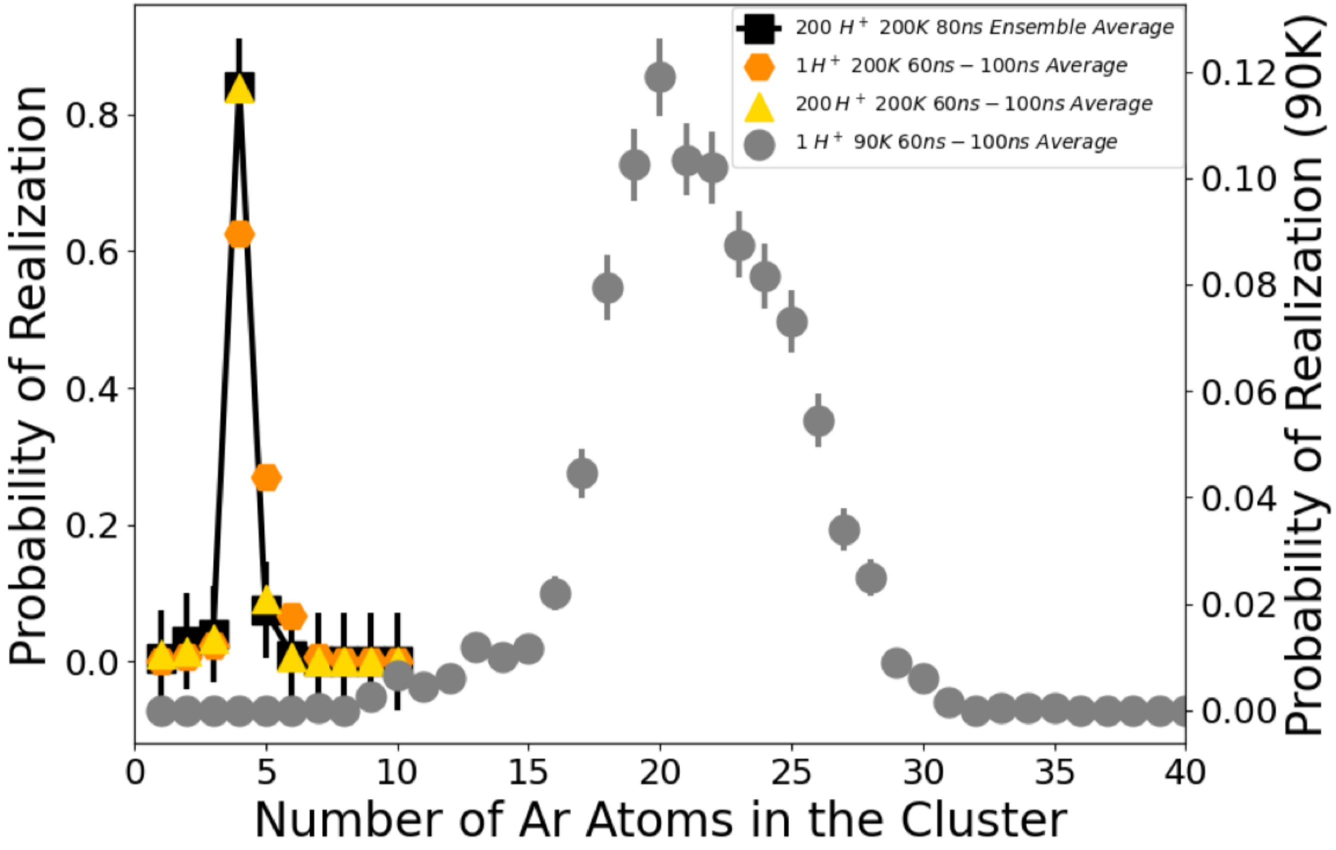

200 H^+ 200K 80ns Ensemble Average
1 H^+ 200K 60ns − 100ns Average
200 H^+ 200K 60ns − 100ns Average
1 H^+ 90K 60ns − 100ns Average
Probability of Realization
Probability of Realization (90K)
Number of Ar Atoms in the Cluster
0.0
0.2
0.4
0.6
0.8
0.00
0.02
0.04
0.06
0.08
0.10
0.12
0
5
10
15
20
25
30
35
40

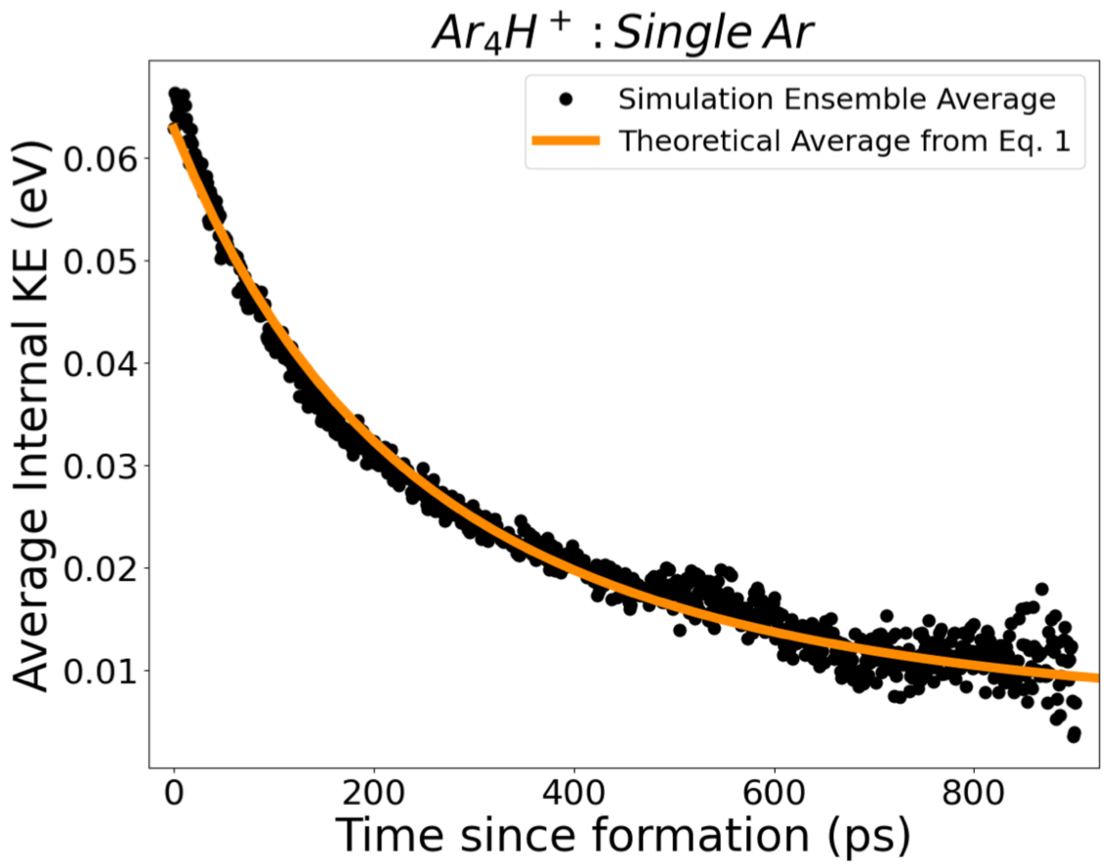

Ar_4H^+ : Single Ar
Simulation Ensemble Average
Theoretical Average from Eq. 1
Average Internal KE (eV)
0.06
0.05
0.04
0.03
0.02
0.01
0
200
400
600
800
Time since formation (ps)

Kinetic Energy in C60 + C60+ Collisions

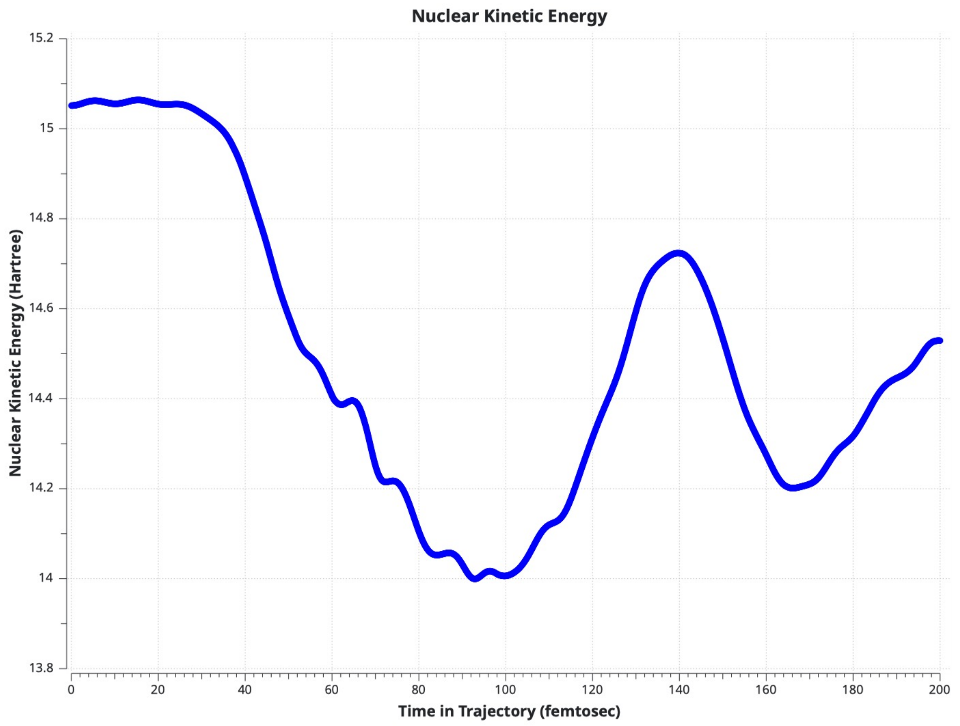

FIGURE 5.6: The nuclear kinetic energy as a function of time taken from one of the QMD simulations of the collision between C_{60} and C_{60}^{+}. This simulation had a collision energy of 409 eVs and an impact parameter of 14.17 a_0.

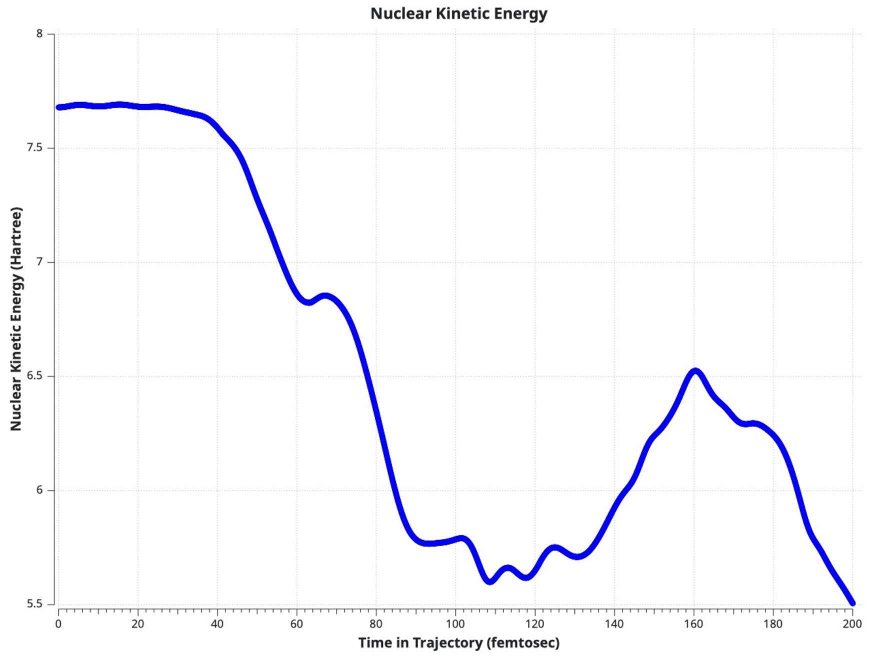

FIGURE 5.5: The nuclear kinetic energy as a function of time taken from one of the QMD simulations of the collision between C_{60} and C_{60}^{+}. This simulation had a collision energy of 200 eVs and an impact parameter of 12.28 a_0.

C60 + C60+   Charge Transfer

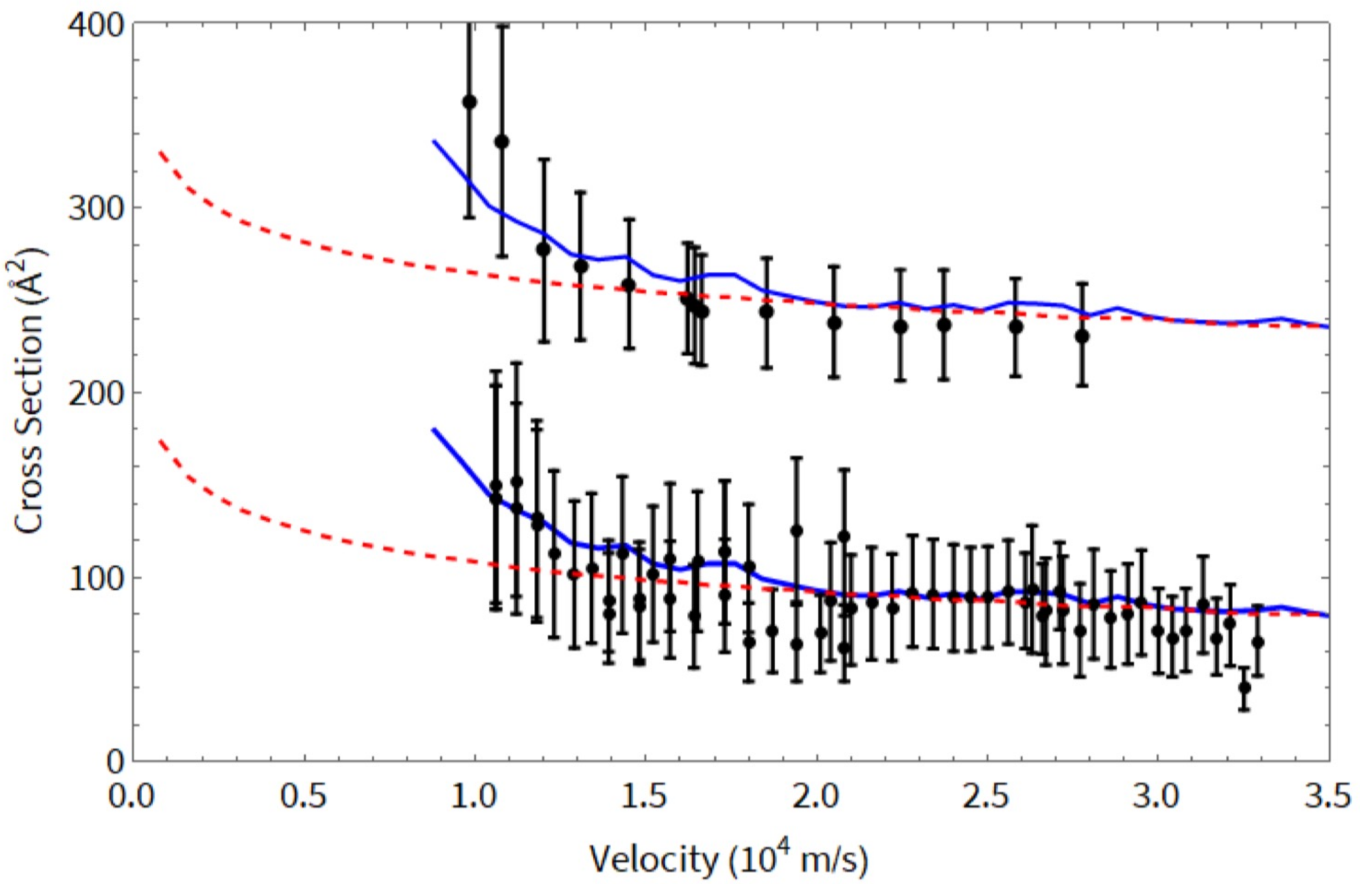

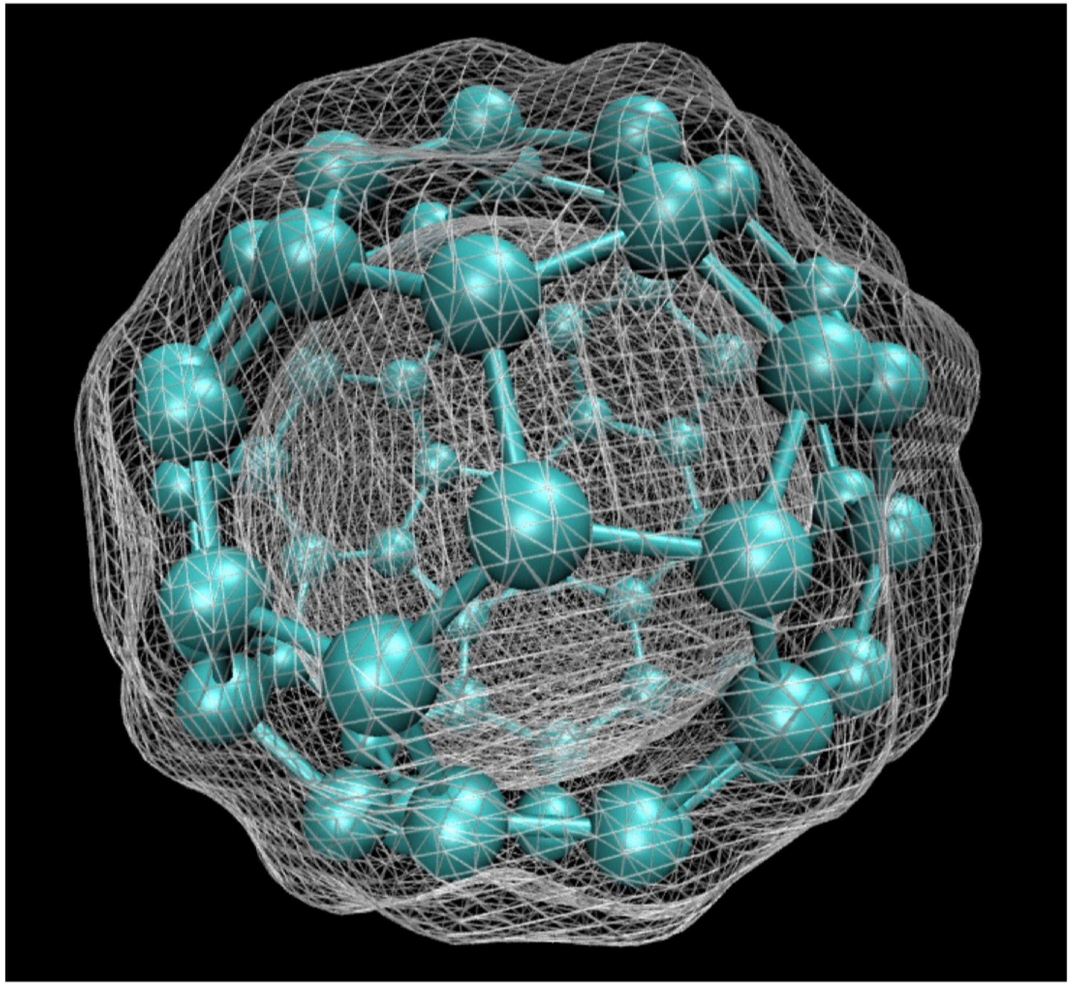

FIGURE 1.1: Geometry of C_{60} and the electron probability isosurface calculated using density functional theory (DFT)[1]

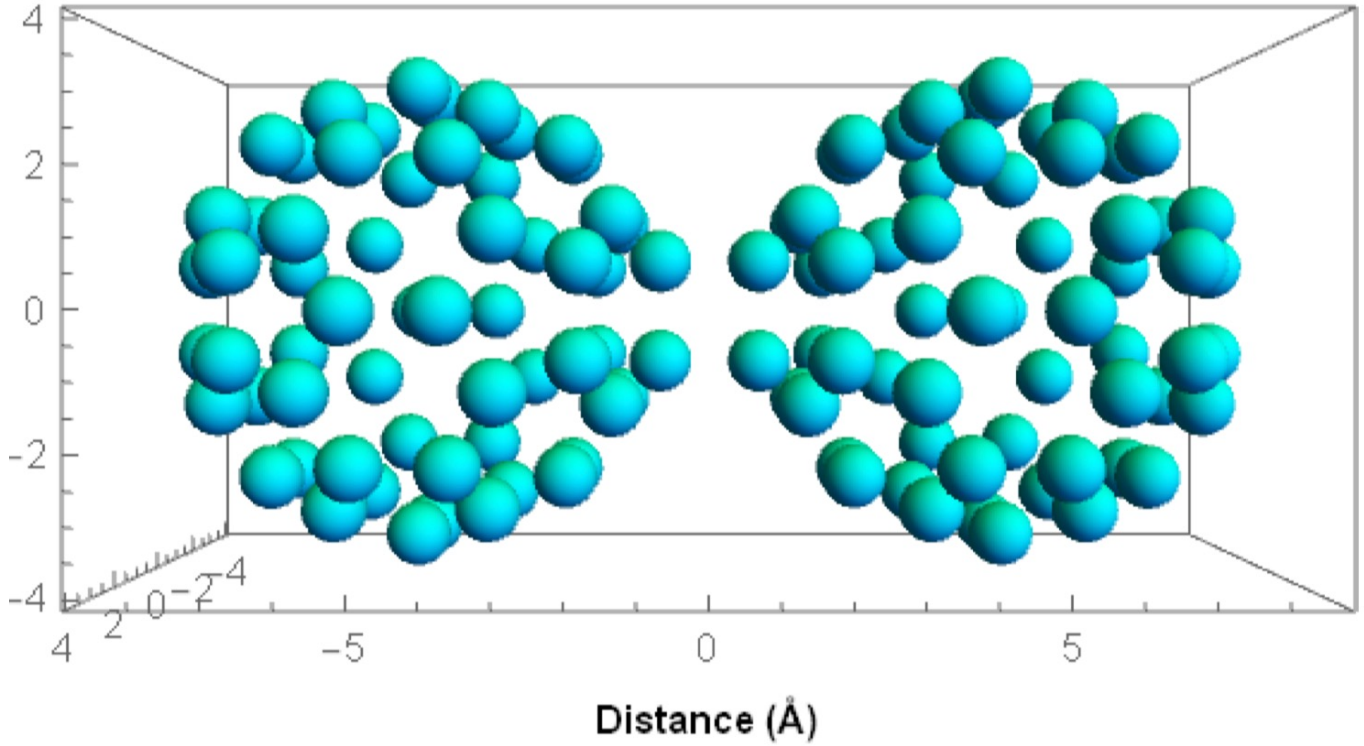

FIGURE 5.3: The optimized geometry for the C_{60} dimer calculated using density functional theory.

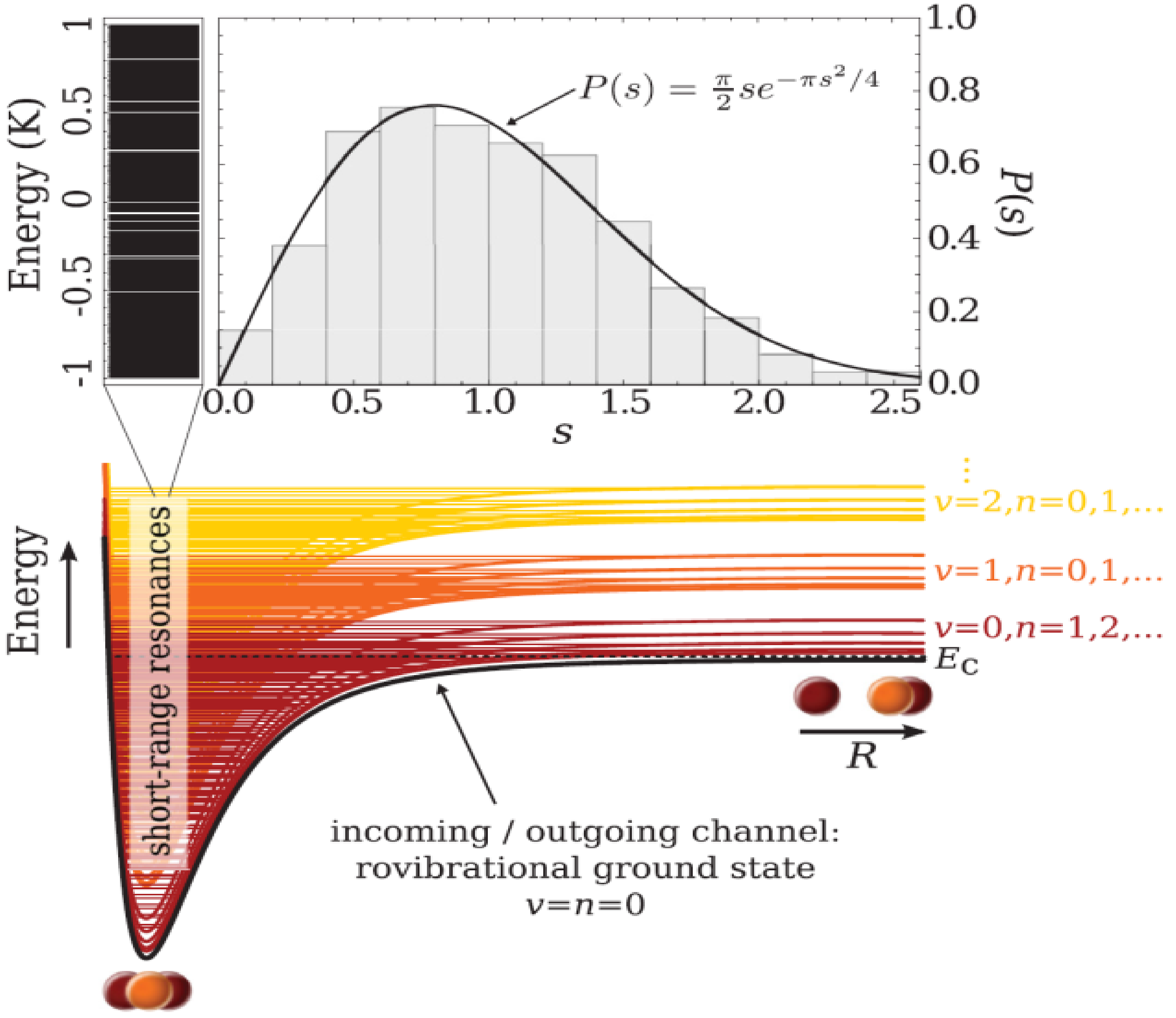

Statistical aspects of ultracold resonant scattering

Michael Mayle, Brandon P. Ruzic, and John L. Bohn
JILA, University of Colorado and National Institute of Standards and Technology, Boulder, Colorado 80309-0440, USA

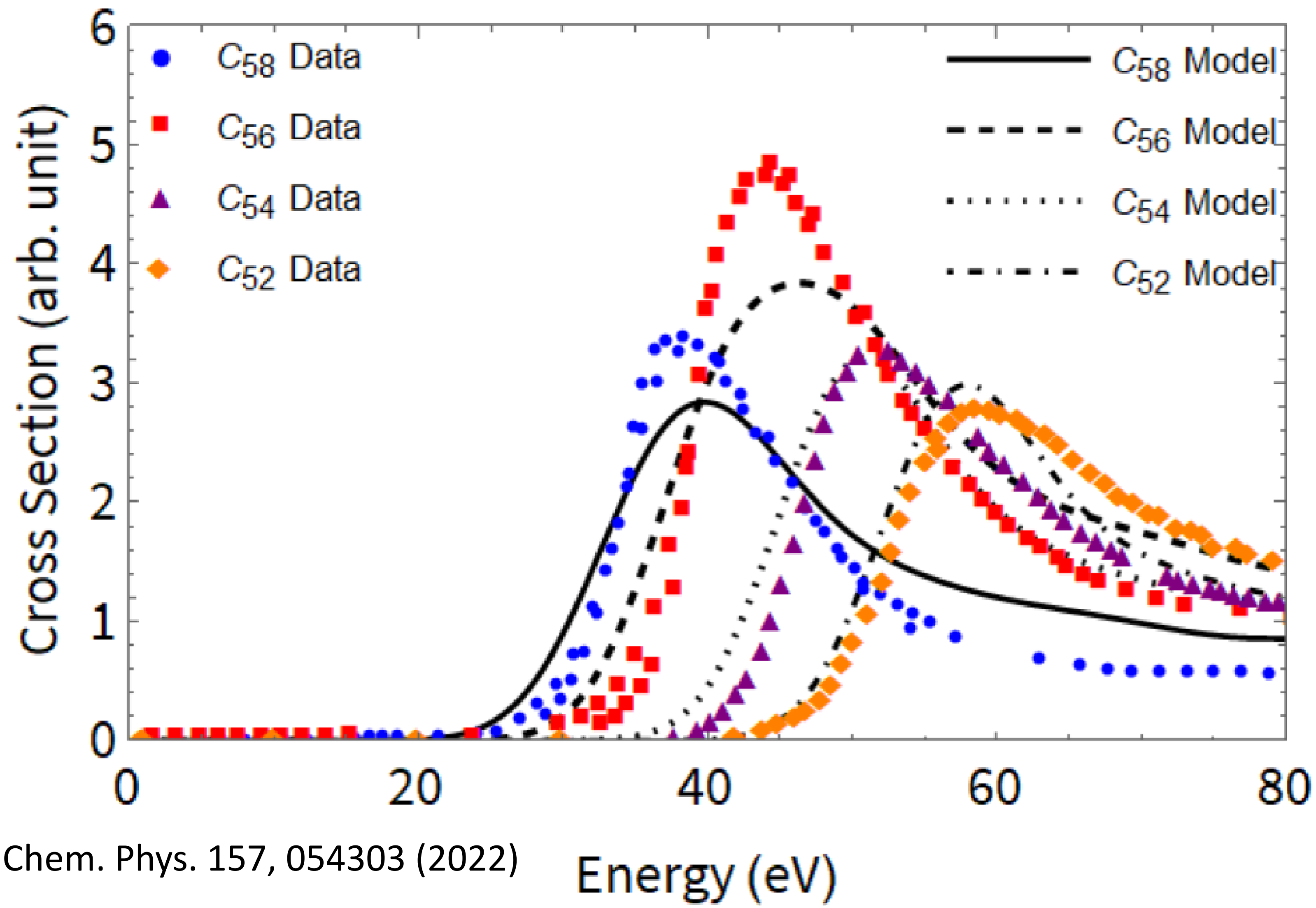

Smucker et. al , J. Chem. Phys. 157, 054303 (2022)

FIGURE 6.8: The experimental cross sections[2] for C_{60} colliding with Ne^+ (shown as the circular, square, triangular and diamond points) plotted along side our model (shown in black).

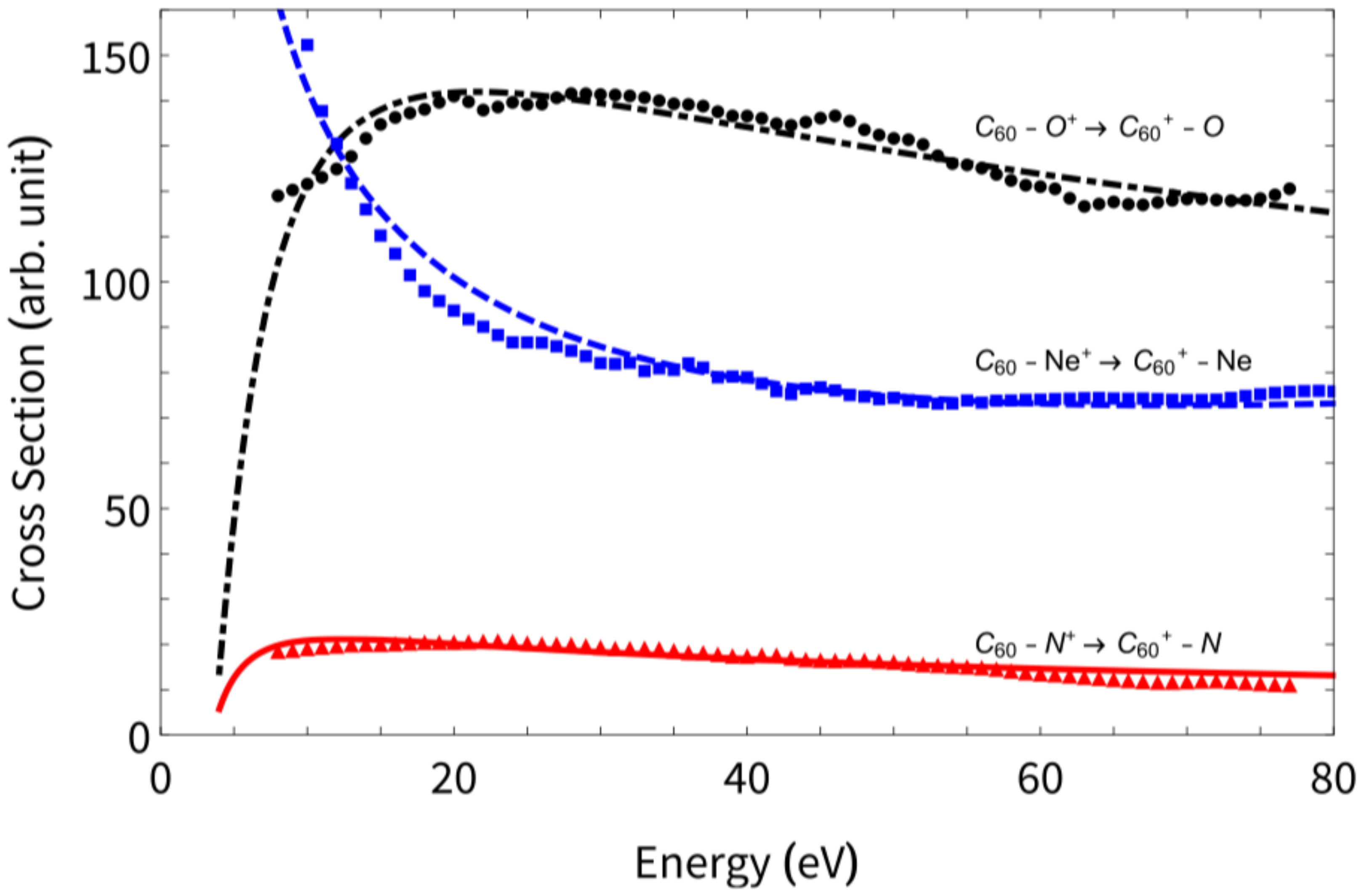

Cross Section (arb. unit)
Energy (eV)
0
50
100
150
0
20
40
60
80
C_{60} - O^+ → C_{60}^+ - O
C_{60} - Ne^+ → C_{60}^+ - Ne
C_{60} - N^+ → C_{60}^+ - N